

SHINING A LIGHT ON GEMSTONE PROPERTIES: AN EXPLORATION OF PHOTOLUMINESCENCE SPECTROSCOPY

Sally Eaton-Magaña, Daniel C. Jones, Rachelle B. Turnier, and Christopher M. Breeding

Photoluminescence (PL) spectroscopy is a powerful testing method for gemstones in which absorption of light leads to emission at longer wavelengths, revealing valuable insights into the material's composition, structure, and optical properties. In gemology, PL is a crucial tool for identifying and characterizing gemstones, understanding their geological history, detecting treatments and synthetics, and providing clues about the presence of impurities, defects, and inclusions.

The advantages and disadvantages of PL will be explored along with a survey of its applications among various gemstones including diamonds, pearls, and chromium-containing gems, with a focus on emerging techniques such as PL mapping, fluorescence lifetime, and large-scale statistical analysis. This article highlights the significance of PL spectroscopy applied to gemstones, revealing new insights into these natural wonders and helping distinguish them from their treated and laboratory-grown counterparts.

Defects that occur within the lattice of a gemstone, due to the disruption of the crystal lattice or the introduction of impurity atoms, often give rise to optically detectable features; these are often called "color centers," "optical centers," "optical defects," or simply "defects." In ionic crystals, the term "F-center" is also used. These defects are a gem's storytellers and can reveal much about its history, whether it formed in the earth or in a laboratory. The atomic-level defects preserved in a gem are determined by its growth conditions as well as any subsequent geological or treatment history.

Gemological laboratories rely on nondestructive analytical techniques, usually based on optical methods such as absorption spectroscopy, Raman, and photoluminescence (PL) spectroscopy. With PL and Raman spectroscopy, a material is exposed to laser light (figure 1), typically under a microscope in a gemological laboratory or research setting, and the resulting emission is measured with a high-resolution spectrometer. PL spectroscopy has become an invaluable

tool in gemological laboratories. This technique is nondestructive and very sensitive, and in some cases it can detect defects at concentrations lower than 10 parts per billion, or ppb (Wotherspoon et al., 2003). The method has numerous applications and can successfully distinguish some treated and laboratory-grown diamonds from their natural counterparts.

In Brief

- Over the last two decades, PL spectroscopy has become one of the most important analytical methods for gemstone identification, particularly diamond.
- PL spectroscopy, closely related to fluorescence as it is also measuring emission from a gem, is capable of detecting defects at very low concentrations that are not measurable by other methods.
- In recent years, specialized technologies such as spatial PL mapping in two and three dimensions, nanosecond-scale lifetime measurements, and large-dataset statistical analysis have become possible and are now being used.

This article provides a historical overview of PL and its applications (see box A), a detailed look at how PL is used in gemology, and an evaluation of

See end of article for About the Authors and Acknowledgments.

GEMS & GEMOLOGY, Vol. 60, No. 4, pp. 494–517,

<http://dx.doi.org/10.5741/GEMS.60.4.494>

© 2024 Gemological Institute of America

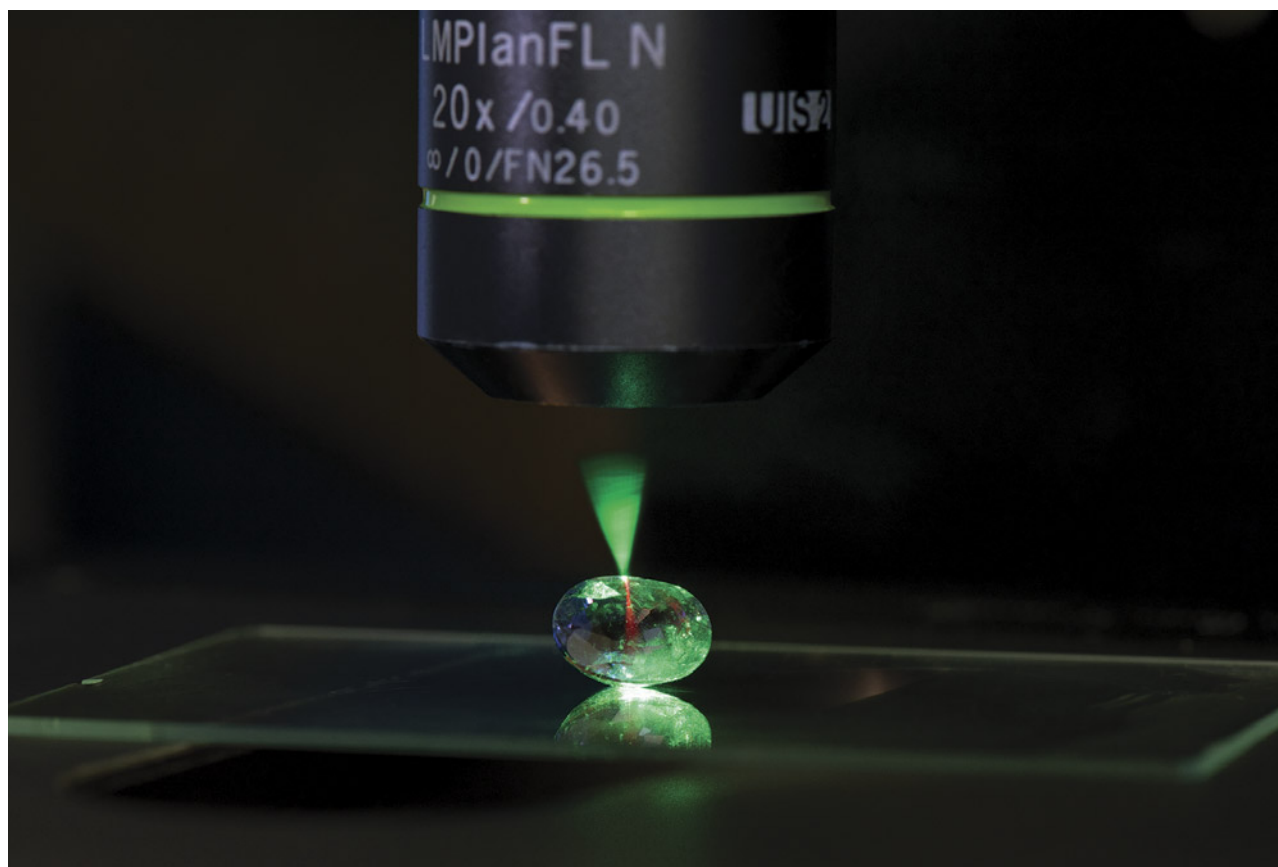


Figure 1. Microscope-assisted photoluminescence spectroscopy is an important technique for collecting data in gemological research and identification. Here, a 514 nm laser illuminates a sapphire sample at room temperature, creating red luminescence caused by trace amounts of chromium. Photo by Kevin Schumacher.

emerging PL-based techniques. For a substantial re-counting of the underlying theory of luminescence (e.g., Nasdala et al., 2004; Waychunas, 2014; Eaton-Magaña and Breeding, 2016; Green et al., 2022; Zhang and Shen, 2023) or a compendium of PL features found in gem materials (e.g., Zaitsev, 2003; Gaft et al., 2015; Hughes et al., 2017; D’Haenens-Johansson et al., 2022), please refer to the cited works.

Impurities in gemstones can produce optical phenomena, resulting in characteristic features or peaks in spectroscopic data. Diamond, for instance, is composed primarily of carbon, but it can contain defects such as vacant lattice sites (i.e., vacancies), displaced carbon atoms (“interstitials”), and elemental impurities such as nitrogen, boron, and nickel atoms. Luminescence features arise from several different mechanisms, including transitions between the material’s intrinsic electronic states, impurities, and structural defects or disorder. These interactions in gems help reveal the defects and the energy states of the atoms involved, making spectroscopy an accurate and useful identification tool in gemology. While

photoluminescence spectroscopy is a more powerful tool than the fluorescence observations that are familiar to those in the trade, both techniques are based on comparable mechanisms and the same emitting defects.

Several important aspects are involved in using PL spectroscopy to detect and identify defects. Along with collecting the spectrum of the emission from the sample (standard PL spectroscopy), additional techniques include (1) cooling the sample to reduce the broadening of spectral features, (2) monitoring photochromic effects, (3) measuring the spatial distribution of the defects across the sample (PL mapping), (4) measuring the fluorescence decay time (time-resolved luminescence, or TRL), and (5) measuring the emission as a function of excitation wavelength (photoluminescence excitation, or PLE). In gemology, technique 1 is regularly used for diamond samples by cooling to liquid nitrogen temperatures (-196°C). Technique 2 can be observed in some PL features due to deep-UV exposure such as with the DiamondView, while techniques 3–5 are only rarely

BOX A: HISTORY OF PL IN GEMOLOGY

Over the past twenty years, PL spectroscopy has become an important tool used by major gemological laboratories to distinguish treated diamonds from their natural counterparts (e.g., Breeding et al., 2010; Lim et al., 2010). Raman analysis, a reliable gem identification tool since the 1930s, employs equipment that is often quite suitable for collecting PL spectra. The application of photoluminescence techniques dates back more than a century, with an early report discussing the photoluminescence of calcite (Nichols et al., 1918). In the latter half of the twentieth century, several dozen articles related to gem materials were published, with most of these focusing on diamond (e.g., Clark and Norris, 1971; Solin, 1972; Walker, 1977; Thomaz and Davies, 1978; Collins et al., 1983b; Collins, 1992; Freitas et al., 1994), along with a few studies on other gem materials such as cinnabar (Simpson et al., 1980), zircon (Shinno, 1987), garnet (O'Donnell et al., 1989), fluorite (Calderon et al., 1990, 1992), forsterite (Glynn et al., 1991), and olivine (Bakhtin et al., 1995).

The adoption of PL spectroscopy as a method of diamond identification began in 1999 when General Electric (GE) announced a high-pressure, high-temperature (HPHT) treatment method for decolorizing type II brown diamonds ("Pegasus Overseas Limited...", 1999; Shigley et al., 1999). Conventional gemological tests could not detect HPHT-treated diamonds, but PL spectroscopy's high sensitivity made identification possible. After the diamond industry's initial alarm following the GE announcement, extensive research showed that PL spectroscopy at liquid nitrogen temperatures was the most

effective method for detecting HPHT treatment (Fisher and Spits, 2000; Smith et al., 2000).

When HPHT treatment was first introduced, detecting the presence or absence of specific PL peaks from a single or a few laser wavelengths was sufficient. If more sophisticated analysis was needed, the tools were not available in the early 2000s. For example, measuring the full width at half-maximum (FWHM, a standard method for determining peak width) was accomplished by the rudimentary procedure of printing out the spectrum and using a ruler. Today, that calculation is performed by standard computer algorithms and, in some cases, performed automatically (e.g., Martineau and McGuinness, 2018). As diamond processing and synthesis have advanced, the standard procedure now demands far greater resources.

Therefore, PL spectroscopy has become a vital addition to all gemological laboratories. Along with the hardware, this technique requires infrastructure such as training and the construction of a spectral database of known samples. In addition to detecting HPHT treatment in colorless diamonds, PL spectroscopy is now used to identify growth history and color origin in both colorless and colored diamonds (Wang et al., 2012). The increasing sophistication of treatment and laboratory growth processes has driven the use of complex analytical methods and instruments, such as mapping spectrometers and automated gem testing, in large gemological laboratories. As a result, PL-related applications have expanded far beyond their original purpose.

applied, typically for research or in an academic setting. Nevertheless, methods 3 and 4 provide important information regarding the identity of defects and will be discussed in greater detail in later sections.

In addition, certain natural and laboratory processes can change the structure of a physical material and hence the PL response. Interpreting PL spectra for some gem materials can reveal permanent treatment such as irradiation and/or annealing, changes or variations in applied stresses of the crystal, changes in the isotopic composition of elements used in laboratory growth, and the implantation and/or diffusion of ions of a known element into the atomic structure. However, using this extensive array of attributes and tests is often not possible due to their unavailability, the cost required, or the destructive nature of the measurement process.

In a gemological laboratory where PL data is being gathered on hundreds or thousands of stones, some

of the considerations during the data collection process include balancing time and data quality, accounting for the heterogeneity of PL features within the gem, and ensuring consistency between gems. The procedure for client stones often consists of collecting PL spectra with one or more lasers of various wavelengths, typically on one location on the stone, and comparing the resulting spectra against a database of known samples.

Although generally utilized by gemological laboratories, PL spectroscopy can also be used by the trade to screen laboratory-grown diamonds and simulants at room temperature using near-UV (385 nm; Tsai and D'Haenens-Johansson, 2021) or deep-UV excitation (193 nm; Wang et al., 2023) and on mounted jewelry pieces (Tsai and Takahashi, 2022; Tsai, 2023). Screening devices can also be employed by trade professionals to collect PL or Raman measurements for the identification of materials such as

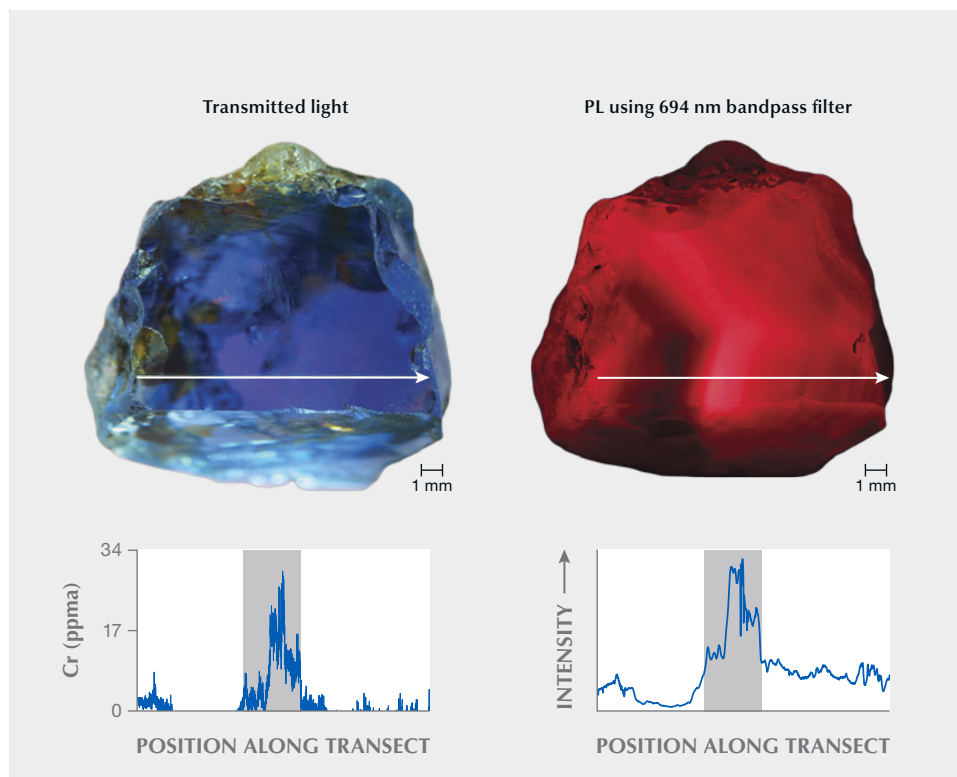


Figure 2. Sri Lankan metamorphic blue sapphire. Left: Shown in transmitted light with an arrow marking a traverse of LA-ICP-MS measurements for chromium. Right: Excited by a 365 nm light source and photographed with a 694 nm bandpass filter attached to a microscope objective, showing the same traverse. The plots show the chromium concentration and PL intensity along the traverse, respectively, with a gray band showing their correlation. Photos by Rachele Turnier.

beryl, corundum, spinel, and zoisite (Culka et al., 2016; Tsai and D’Haenens-Johansson, 2021). Recent advancements have made PL systems available at a lower cost than full laboratory-grade instruments, assisting the industry in detecting fraudulent gems. While the results may not conclusively determine whether a diamond is natural, treated, or laboratory grown, they can provide helpful screening and identification.

Advantages. One of the hallmarks of PL spectroscopy is the sensitivity it can achieve. It can detect optical peaks indicating concentrations at the ppb level (Iakoubovskii et al., 2001; Wotherspoon et al., 2003). These highly sensitive instruments can identify dozens to hundreds of peaks depending on the material, which can help create a reliable database of distinguishing characteristics for natural, treated, and laboratory-grown gemstones. This sensitivity is generally unmatched by other noninvasive, nondestructive methods, making PL analysis vital for gem identification (Hainschwang et al., 2024).

For example, even in diamonds with no detectable nitrogen impurities by infrared absorption instruments (i.e., type II diamonds; below the detection limit of ~1–5 ppm), PL spectroscopy can detect

NV concentrations of 10 ppb or less (Wotherspoon et al., 2003). Therefore, the type II designation does not mean an “absence of nitrogen,” but rather that the diamond contains very low concentrations of this impurity. Nitrogen-containing defects (such as H2, H3, H4, N3, and NV centers) are usually the dominant features in the PL spectra of type IIa diamonds. Similarly, in corundum the efficiency of Cr³⁺ luminescence allows concentrations in the ppb range to be detected in sapphires. This is advantageous for using PL maps to characterize chromium zoning in corundum (e.g., figure 2).

With PL spectroscopy, several features in diamond not seen by ultraviolet/visible/near-infrared absorption spectroscopy may be detected consistently due to higher sensitivity (e.g., figure 3). The technique offers not only high detection sensitivity but also high spatial sensitivity when PL measurement is used in conjunction with a microscope, making it possible to create concentration maps showing the spatial distribution of defects (Loudin, 2017) or other parameters such as internal strain (Noguchi et al., 2013). Unlike the visible and infrared absorption measurements typically used in gemological laboratories, which are bulk measurements, PL spectroscopy can perform point measurements and control the activation volume of the material. This

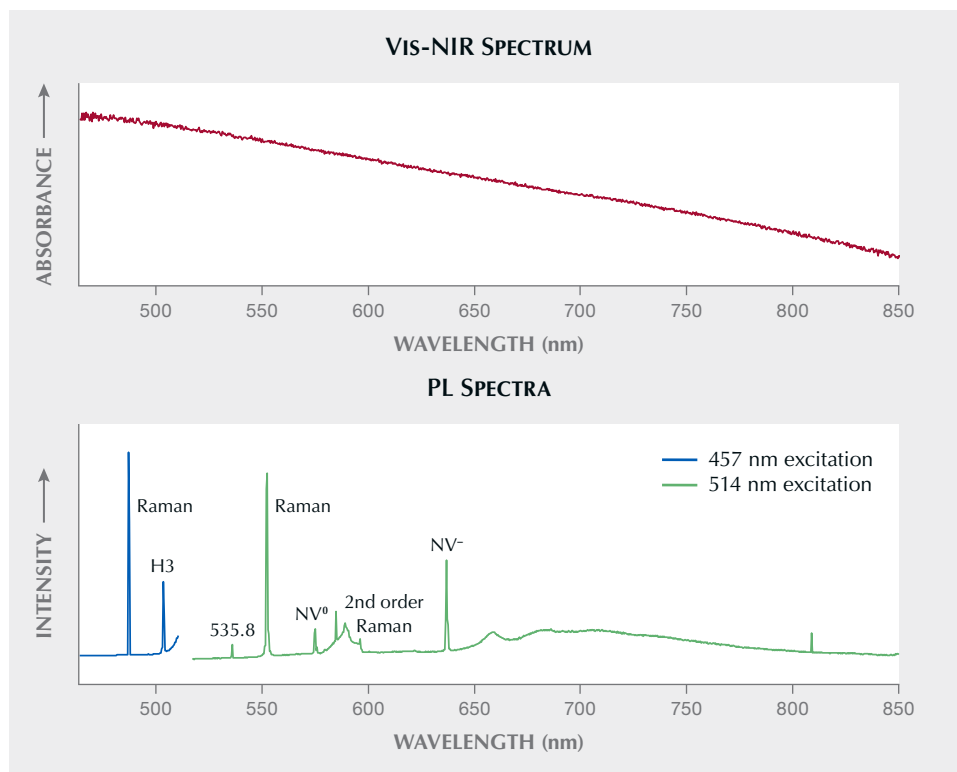


Figure 3. Spectroscopic data for a 10.09 ct H-color type IIa HPHT-treated diamond collected at liquid nitrogen temperature demonstrate the enhanced sensitivity of PL spectroscopy for detecting defects. While the Vis-NIR absorption spectrum is featureless (top), the PL spectra (bottom) show Raman features that identify the sample as diamond along with numerous peaks that aid in identification. Note that the wavelength of Raman lines shifts with the laser excitation wavelength, causing the positions of the diamond Raman lines to differ for spectra collected with 457 and 514 nm excitation.

spatial ability will be discussed further in the section on PL mapping.

PL spectroscopy also has the advantage of not requiring any sample preparation beyond cleaning, and spectra can be collected from rough surfaces as well as irregularly shaped samples such as pearls and carvings. While spectra can be collected from rough surfaces, surface topography does affect the intensity of a PL feature. Thus, PL maps collected from rough samples will show variations in PL intensity that correlate with cracks or surface height, superimposed on PL variations related to changes in defect concentration.

Disadvantages. While PL spectroscopy offers significant advantages, there are also important disadvantages to consider. For high-quality spectra, there are correspondingly high costs. Most PL systems have specialized microscopes, lasers, and spectrometers, costing hundreds of thousands of U.S. dollars along with significant maintenance costs (approximately 10% of the purchase cost annually). While small desktop and portable versions using charge-coupled devices (CCDs) offer some of the features of more expensive systems, they may fall short in other areas such as spectral resolution (the ability to distinguish individual peaks) or spatial resolution (distinguishing variations across a sample).

Operating the device typically requires specially trained users who are knowledgeable about the theory and instrumentation and can ensure that spectra are correctly collected. Operators must also be trained in special safety protocols. Although the devices are generally operated within an enclosure and designated as safe Class I lasers, laser safety training is essential, as is knowledge of safe cryogenic handling when working with diamonds at liquid nitrogen temperatures.

Temperature plays an important role in PL analysis of diamonds, particularly in cooling samples to liquid nitrogen temperatures. The PL features of diamond defects become more pronounced at these very low temperatures. Higher temperatures can reduce, shift, broaden, or eliminate their response. The effect of temperature can be clearly seen in the PL spectrum of a near-colorless, type IIa diamond shown in figure 4 at temperatures ranging from ~80 K (–193°C) to room temperature.

Unlike most gemstones, diamonds can be cooled to liquid nitrogen temperatures to optimize PL spectroscopy results because of their low coefficient of thermal expansion and very high thermal conductivity. Other gems (and heavily included diamonds) have a much greater risk of shattering when cooled. For example, corundum has a coefficient of thermal

expansion five times higher than that of diamond (Fiquet et al., 1999), while its thermal conductivity is 65 times lower (Read, 2008).

Only optically active defects that emit light can be detected with this method, and their detection depends on operating conditions such as temperature, excitation laser, and light wavelength. These limitations affect the detection of all impurities and defects in the stone. For example, Lai et al. (2020) used PL spectroscopy to show that high-pressure, high-temperature (HPHT) annealing of some natural diamonds revealed the creation of previously undetectable SiV⁻ defects that produce luminescence at 737 nm. The silicon impurities had been present

but were not detected because they existed in a form that was not optically active. They required HPHT annealing to transform into optically active centers indicating the presence of silicon. Similarly, boron-related peaks such as the 648.2 nm (B_i) and 776.4 nm (ascribed to a boron-vacancy complex) PL features can be created at moderate annealing temperatures and annihilated at higher temperatures (Green, 2013; Eaton-Magaña and Ardon, 2016). In diamonds where these features cannot be detected and uncompensated boron is not detected by IR absorption spectroscopy, the presence of boron impurities generally cannot be known without chemical analysis. Therefore, PL analysis can often provide a

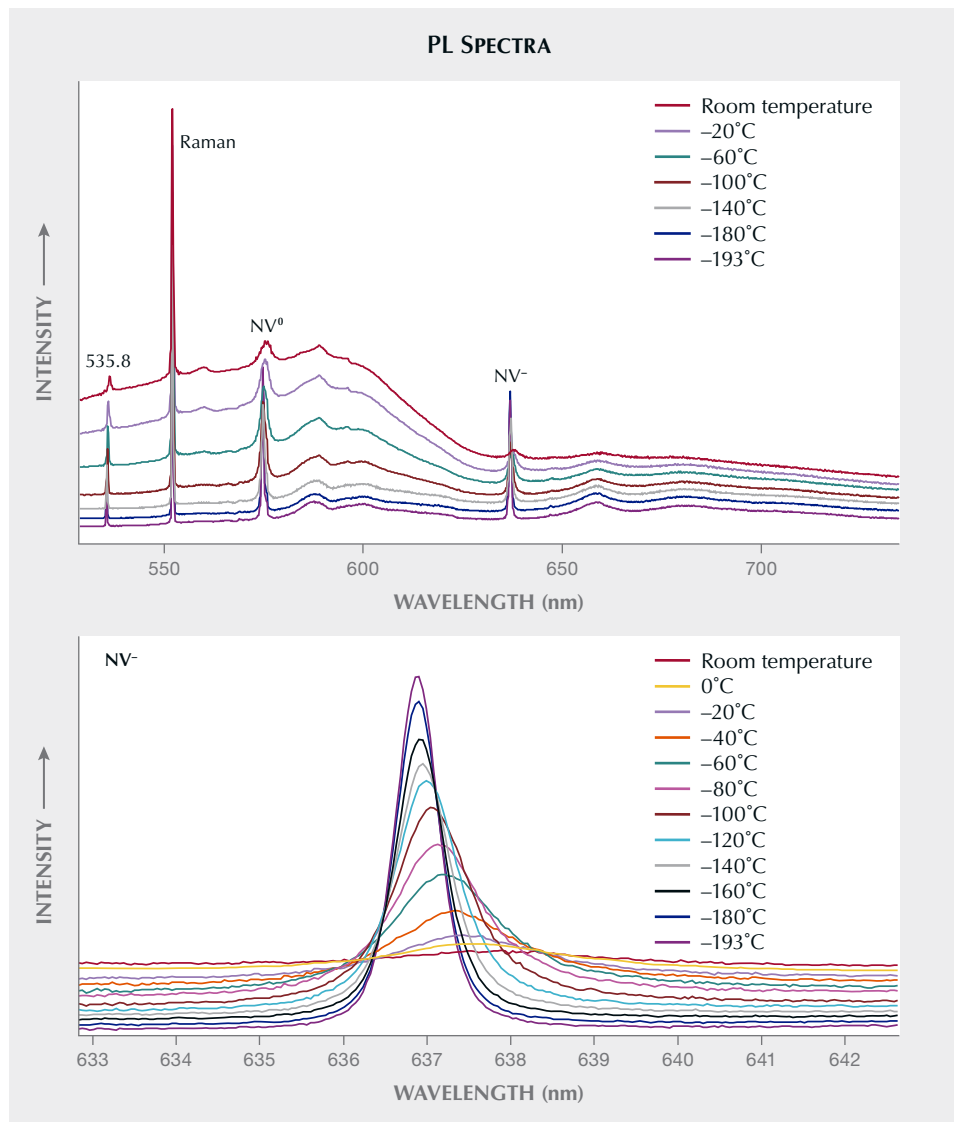


Figure 4. Temperature effect on the 514 nm PL spectra of a near-colorless type IIa diamond from liquid nitrogen temperature to room temperature (-193° to 23°C) across a broad wavelength range (top) and for the NV⁻ defect (bottom). The NV⁻ peak is well-defined at low temperature but broadens and decreases in intensity with increasing temperature, becoming much weaker at room temperature. Spectra are offset vertically for clarity and intensities are scaled to the Raman peak.

good indication of impurities in diamonds, but some impurities may go undetected because they are not optically active and can only be identified through destructive tests.

Distinction Between Raman and PL Spectroscopy.

Raman spectroscopy is a crucial tool for evaluating and identifying many gems (Bersani and Lottici, 2010; Kiefert and Karampelas, 2011; Groat et al., 2019; Smith et al., 2022; Jin and Smith, 2024, pp. 518–535 of this issue). While instruments configured to detect PL features often detect Raman peaks as well, there are several important differences between these two types of peaks. Photoluminescence emits from a material at a constant energy (or wavelength). For example, the NV⁰ defect can, with NV⁻, give diamond a pink to orangy pink bodycolor. It has principal absorption and emission at 575 nm, regardless of the nature or the wavelength of the excitation source. The absorption band and the luminescence band do not shift to different wavelengths simply because a different light source is used.

In contrast, the energy *difference* between the Raman peak and the excitation wavelength is constant. Consequently, the absolute energy of the scattered photons depends on the energy of the photons in the excitation source, and so the wavelength of a Raman peak is not constant and varies with the excitation source. In Raman spectroscopy, light interacts with the molecular vibrations, or phonons, of the material. This causes a change in frequency because the material reemits the absorbed light; the resulting peaks indicate the energy change caused by these vibrational (and sometimes rotational) energy levels.

Although this vibrational energy shift occurs in only one out of 10 million photons coming from the sample (Berry et al., 2017), the Raman peak is the dominant feature in most PL spectra of type IIa diamonds. This highlights the very low intensity of the luminescence peaks in type IIa diamonds and the need for very sensitive equipment to accurately measure the PL properties. On the other hand, chromium or iron impurities in corundum can hinder the collection of Raman spectra by producing PL bands that overlap with Raman peaks. Careful selection of laser wavelength is thus an important consideration during experimental design—for example, choosing a blue excitation wavelength to avoid overlap between Cr³⁺ and Raman bands in corundum (Nasdala et al., 2004, 2012; Zeug et al., 2017).

A Raman spectrum can identify a stone as diamond, but the PL spectrum provides additional in-

formation that an experienced analyst can interpret to determine if the diamond is natural, treated, or laboratory-grown. Both methods have an important place in gemology: Raman for identifying a material and PL for further evaluating the stone's history. Importantly, the diamond Raman line and the PL features appear in the same spectrum, originating from the same sample volume and dependent on similar laser power (Collins, 1992). This allows semiquantitative comparison of PL features corresponding to lattice defects in different spectra by ratioing the integrated intensity of the PL peak to the area of the diamond Raman line (though the values can still be affected by the presence of other point defects that compete for the laser excitation or quench the luminescence). This normalization procedure is helpful in comparing PL features between samples, after different treatments, or in comparing spatial variations across the gem. Normalization is especially important in cases of mapping rough materials where spatial variations may be obscured when surface topography creates variations in peak intensity.

Effect of Different Excitation Wavelengths of Lasers.

Many lasers in the UV-Vis-NIR wavelength range are now necessary, as different laser wavelengths effectively activate different PL features. Common laser excitation wavelengths include 325, 355, 405, 455, 457, 488, 514, 532, 633, 785, and 830 nm for single-point spectroscopy and PL mapping, but any commercially available laser wavelength can be used for either if the necessary laser filters are available. The use of multiple laser wavelengths maximizes the number of PL peaks that can be detected, since certain peaks are more effectively excited by particular wavelengths. Furthermore, some peaks may be obscured at a specific excitation if stronger features occur at a similar wavelength (figure 5).

GEMOLOGICAL APPLICATIONS

Natural Diamond. Aside from nitrogen, boron, hydrogen, nickel, and silicon, few other elements are regularly incorporated into natural diamond due to the high atomic density and charge states of diamond. Nevertheless, this small set of diamond-compatible elements creates a wide range of optical transitions (e.g., Zaitsev, 2001; Ashfold et al., 2020; D'Haenens-Johannson et al., 2022).

All type II diamonds, either D-to-Z or fancy-color, now require low-temperature PL analysis to reliably verify them as natural, treated, or laboratory-grown.

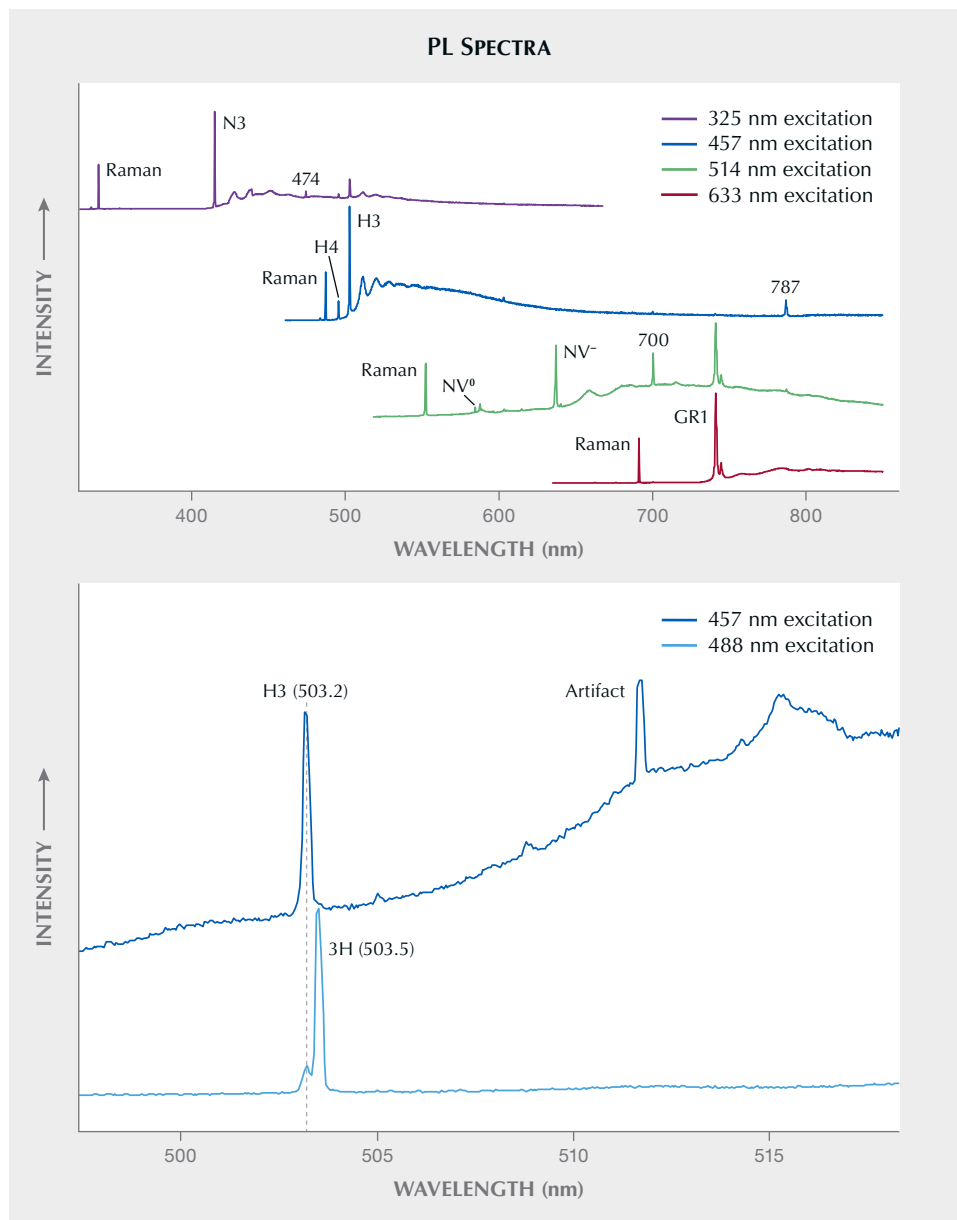


Figure 5. Top: PL spectra of a 1.16 ct Fancy green-gray natural diamond. Across the array of lasers, several peaks are more efficiently detected with one laser over another. For example, NV⁻ centers are best observed with 514 nm excitation, GR1 with 514 and 633 nm excitation, and H3 with 457 nm excitation. The N3 peak could only be detected with the 325 nm laser. Bottom: A 1.10 ct D-color natural diamond shows distinctive features even with lasers of slightly different wavelengths. The H3 peak at 503.2 nm is detected with 457 nm excitation, while the 488 nm laser can detect both the H3 and the 3H peak at 503.5 nm. Spectra are offset vertically for clarity, and the Raman peaks are scaled as equal.

All type IaB diamonds with low nitrogen also require low-temperature PL spectroscopy to distinguish natural color from treated color. For example, type IIa pink and type IIb blue natural diamonds are quite rare, with prices sometimes exceeding US\$1 million per carat. The natural origin of such diamonds is almost always confirmed by their PL spectral characteristics.

PL spectroscopy has been useful in characterizing natural diamonds for a wide variety of fundamental research applications. For example, it helps characterize gems from specific geographic locations (Ko-

marovskikh et al., 2020) and from unusual formations such as impact diamonds found in meteor craters (Yelissev et al., 2016). Another key application is characterizing PL features associated with optical centers such as boron (Lu et al., 2017), the 550 nm absorption band (Eaton-Magaña et al., 2020), and the 480 nm absorption band (Lai et al., 2024a).

Treatment Identification of Gem Diamond. HPHT Treatment. The origin of a diamond (whether mined from the earth or manufactured in a laboratory) and

its subsequent processing are significant factors in a diamond's value. HPHT treatment, regardless of its complexity, is generally quite short (lasting from minutes to hours). The time needed for defects to re-arrange in a natural diamond while it resided in the earth at $\sim 1050^{\circ}$ – 1250°C (Stachel and Luth, 2015) simply cannot be replicated in a laboratory. Therefore, higher treatment temperatures are used to compensate for the shorter time available compared with natural diamonds. These higher temperatures (1800° – 2100°C at 5–6 GPa confining pressure) can also create PL features that are telltale signs of the treatment.

While many of the identifying features detected by PL spectroscopy go undisclosed due to proprietary concerns, some have been published. It has been widely reported (e.g., Fisher and Spits, 2000) that after HPHT treatment, the intensity of the PL peak at 637 nm (NV^-) is often stronger than its 514 nm laser-excited counterpart at 575 nm (NV^0). For most natural type II diamonds, this relationship is reversed (figure 6). Under the temperature conditions required to remove the brown color, HPHT treatment typically breaks down the nitrogen aggregates to form isolated nitrogen impurities that act as electron donors. The charge transfer of new electrons causes an increase in the PL intensity of the 637 nm defect compared to the 575 nm peak (Chalain et al., 2000); therefore, most HPHT-treated type IIa diamonds have an intensity ratio of $I_{637}/I_{575} > 1$. Some of the individual vacancies that make up the NV centers are also thought to be liberated from vacancy clusters decorating slip planes during the treatment.

Combined Processed Diamonds. The introduction of HPHT treatment in the late 1990s brought about treatments that combine HPHT annealing with subsequent treatments such as irradiation and lower-temperature annealing. This “stacking” of treatments, often with the intent to obscure earlier color treatment, can make identification more difficult and make the diamond appear more spectroscopically “natural.” Multi-treatment processes can also be used to create certain attractive colors such as pink to red. Identifying treated diamonds often requires a combination of advanced testing techniques. It is increasingly important to consider the presence or absence of numerous PL features in addition to information from other spectroscopic and gemological techniques such as UV-Vis-NIR absorption, deep-UV fluorescence imaging, and microscopy. For many high-value diamonds, PL spectra are often the most important piece

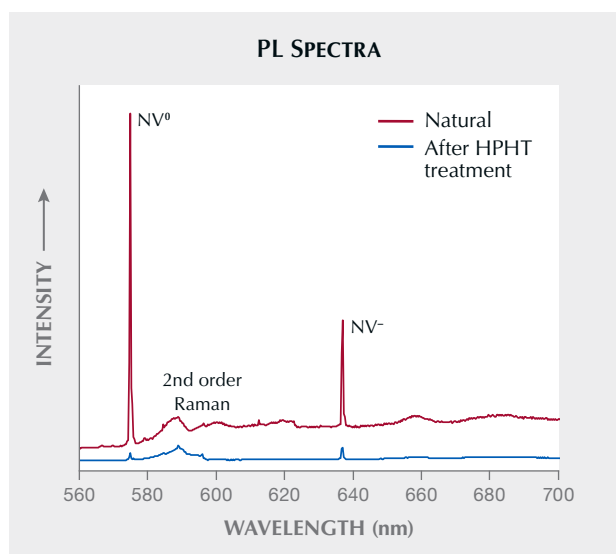


Figure 6. These two PL spectra with 514 nm excitation were collected before and after HPHT treatment of a type IIa diamond. The HPHT treatment caused a reduction in the NV intensities but also shifted the ratio of NV^-/NV^0 from values < 1 to > 1 . The natural diamond weighed 3.07 ct with L color. After treatment, it weighed 3.04 ct with E color.

of evidence, but all tests and data must tell a consistent story. Therefore, gemologists cannot rely solely on a single property or technique. With complex treatments and the evolution of synthetic diamond growth techniques, the accurate assessment of color origin is best left to fully equipped gemological laboratories with knowledgeable, experienced staff.

Laboratory-Grown Diamonds. In recent years, gem-quality laboratory-grown diamonds produced by either chemical vapor deposition (CVD) or HPHT methods have become widely available on the market (Eaton-Magaña and Shigley, 2016; Eaton-Magaña et al., 2017). High-quality PL spectroscopy has proven useful for their identification (e.g., Wang et al., 2007, 2012; Song et al., 2012; D’Haenens-Johansson et al., 2022; Johnson et al., 2023). The rapid development of CVD synthesis techniques over the past two decades has made PL spectroscopy important for accurately verifying CVD origin and detecting post-growth annealing (Hardman et al., 2022b). Impurities rarely found in natural type II diamonds such as nickel (as the 883/885 nm doublet when measured at liquid nitrogen temperature) and silicon (as SiV^- with a 736.6/736.9 nm doublet when measured at liquid nitrogen temperature or as SiV^0 with a zero-phonon line [ZPL] at 946 nm) are often detected in

HPHT-grown and CVD-grown diamonds, respectively. Other PL features, such as the uncharacterized PL peak at 468 nm, are often detected in CVD-grown diamonds (e.g., Zaitsev et al., 2021).

Spinel. PL spectroscopy is most commonly used with diamond analysis, but it has important applications for other gemstones as well. For example, it can be very difficult to distinguish high-clarity natural and laboratory-grown spinel using standard gemological methods. However, synthetic spinel can be distinguished through PL analysis of chromium luminescence (Deeva and Shelementiev, 2002; Kitawaki and Okano, 2006). Natural spinel exhibits a strong ZPL at ~686 nm, along with several other narrow peaks, while their laboratory-grown counterparts show significantly broadened and shifted peaks.

Additionally, PL spectroscopy is helpful in identifying treatment. Sharp chromium peaks verify that the stone is natural and unheated, while heat treatment typically broadens and shifts the position of the PL peaks (Saeseaw et al., 2009; Kondo et al., 2010; Malsy et al., 2012; Liu et al., 2022; Wu et al., 2023).

Corundum. Research on photoluminescence in corundum has been driven by the physics and materials science communities, spurred by the use of corundum as laser crystals (ruby and titanium-doped sapphire). Studying PL in corundum is much more complex than in diamond due to the variety of potential trace element impurities and the difficulty of isolating and identifying the source of various PL bands. The most well-studied emission is Cr³⁺ in corundum, seen as a series of sharp peaks at 692.8 and 694.2 nm, called the R1 and R2 or “R-lines,” short for “Raman lines.” These are sometimes accompanied by sidebands called N-lines, short for “neighbor lines,” in corundum with higher chromium concentrations (Gugushev et al., 2010). Cr³⁺ is very efficient at generating visible luminescence in corundum, even at chromium concentrations around a few ppma (Hughes et al., 2017). Due to the sensitivity of chromium luminescence and the potential for chromium concentrations to vary during the growth of a corundum crystal, PL mapping of the 694 nm luminescence band can reveal internal growth textures. Chromium luminescence is notably quenched by iron impurities (e.g., high-iron rubies with diminished fluorescence). Other trace element substitutions with absorption bands that overlap with either chromium luminescence wavelengths or

the excitation wavelength may also affect the resulting luminescence (Yu and Clarke, 2002).

Other luminescence bands in natural corundum are less extensively characterized. The presence of Mn⁴⁺ can be seen as a sharp peak at ~678 nm, which increases in intensity with manganese content until an inflection and exponential decrease after 0.1 wt.% manganese (Ivakin et al., 2003). A broad band with a peak at 740 nm is thought to be due to Ti³⁺ luminescence (Mikhailik et al., 2005). But different titanium valence states have different luminescence signatures. When Ti⁴⁺ substitutes for a vacant Al³⁺, interactions between Ti⁴⁺ and O²⁻ result in blue to chalky white luminescence. Lower concentrations of Ti⁴⁺ result in a blue band peaking around 415 nm that shifts to longer wavelengths and whiter luminescence as Ti⁴⁺ concentrations increase (Wong et al., 1995). This luminescence is rarely seen in natural sapphire because of other divalent trace elements that charge-balance Ti⁴⁺ (e.g., the Fe²⁺-Ti⁴⁺ charge transfer that causes blue coloration in sapphire) and the overlapping charge-transfer band of Fe³⁺, which is usually present in much greater concentrations compared to Ti⁴⁺ and is known to quench luminescence. Heat-treated sapphire usually shows blue to chalky white luminescence because the dissolution of rutile silk introduces excess Ti⁴⁺, except in high-iron sapphire where Ti⁴⁺ pairs with iron rather than occurring as isolated Ti⁴⁺ that can pair with O²⁻ (Hughes et al., 2017). The prevalence of blue to chalky white luminescence in heat-treated corundum and its rarity in untreated corundum make this an important line of evidence for heat treatment. A lesser-studied luminescence band is orange or “apricot”-colored luminescence, likely caused by the combination of F-centers and divalent ions (e.g., Mg²⁺) in sapphires with iron concentrations <1000 ppm (Vigier et al., 2024). Orange luminescence can occur in all colors of natural or synthetic sapphire and almost all beryllium-diffused corundum (Fritsch et al., 2011).

Pearls. After diamond, pearls are the gem most commonly analyzed using PL spectroscopy. PL features in pearls are generally attributed to organic compounds within the nacre composite material (Karampelas et al., 2007). This technique, especially using a 514 nm laser, makes it possible to distinguish naturally colored pearls from artificially colored pearls (e.g., Wang et al., 2006; Karampelas et al., 2011). This is true for both natural and cultured pearls, as the treatment creates notable differences

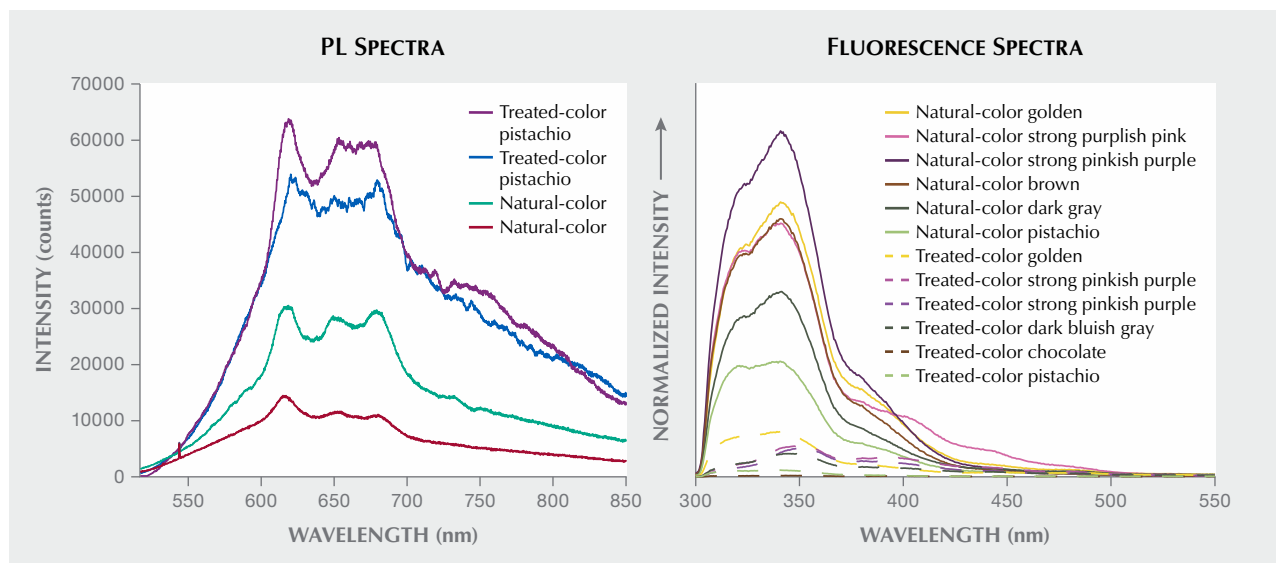


Figure 7. Left: PL spectra obtained for two color-treated “pistachio” pearls and two naturally colored specimens using 514 nm laser excitation. The characteristic feature at around 650 nm becomes less defined in the treated cultured pearls (Zhou et al., 2016). Right: Fluorescence spectra of naturally colored and color-treated pearls (Tsai and Zhou, 2020).

in PL spectra (e.g., figure 7; Zhou et al., 2016; Tsai and Zhou, 2020).

PL spectroscopy can also detect a series of bands positioned at 620, 650, and 680 nm, attributed to porphyrin pigments (Iwahashi and Akamatsu, 1994; Karampelas et al., 2020). These pigments are responsible for the natural gray to black tones in pearls produced by mollusk species such as *Pinctada margaritifera* and *Pteria* species. These bands are lacking in dark-colored pearls dyed with silver nitrate.

Treated “chocolate” and “pistachio” pearls from *P. margaritifera* have been modified from their original gray to dark gray color by a series of chemical and physical processes. These treated pearls retain some porphyrin characteristics in their PL spectra, but the features are less defined and show a higher overall fluorescence intensity (i.e., their F/A ratio). This ratio compares the highest fluorescence intensity in the 600–700 nm region to the main aragonite Raman peak at 545 nm or Raman shift of 1085 cm^{-1} (e.g., figure 7, left; Zhou et al., 2016). In a study on golden South Sea cultured pearls, the broadband fluorescence detected by PL spectroscopy (with a high F/A ratio) effectively separates naturally colored from dyed cultured pearls (Zhou et al., 2012).

Fluorescence spectroscopy using a long-wave UV (385 nm) light-emitting diode (LED) excitation provides a quick and effective method to detect optical

whitening and brightening of pearls (Zhou et al., 2020). Short-wave UV (275 nm) LED excitation is used to measure fluorescence features attributed to the amino acid tryptophan within a pearl’s nacre (Tsai and Zhou, 2021). Naturally colored and unprocessed pearls show fluorescence signals at least 2.5 times stronger in the UV region compared to treated or processed pearls (e.g., figure 7, right; Tsai and Zhou, 2020).

Other Gemstones. PL methods have benefited fundamental research and identification issues for a number of gems. Chromium-related PL has been useful for gemstones including topaz (Zeug et al., 2022), gahnite (Chen et al., 2024), and emerald. In particular, the position of the R1 line at ~684 nm due to chromium (Thompson et al., 2014, 2017; García-Tolosa et al., 2019) is key to distinguishing various origins of emerald. In laboratory-grown emerald, this line is located at shorter wavelengths, and natural emeralds from a non-schist environment have an R1 line position that is comparable. Meanwhile, natural emeralds with schist origins have an R1 position at higher wavelengths (Thompson et al., 2014). This R1 line, particularly when combined with other gemological information, has also proven useful in geographic origin determination between several sources such as Colombia, Afghanistan, and Zambia (Thompson et al., 2017).

PL spectroscopy has been instrumental in detecting other defects measured in gemstones such as the iron-related emission in feldspar (Prasad and Jain, 2018) and irradiated kyanite (Nagabhushana et al., 2008). PL detection is also useful in zircon for detecting rare earth elements (REEs; Vuong et al., 2019) or measuring the transition of crystalline to metamict zircon due to irradiation damage (Lenz et al., 2020).

PL spectroscopy has also proven helpful in the characterization of some organic gems beyond pearls. Paired with Raman spectroscopy, the interpretation of PL spectra can distinguish natural red coral from dyed coral (Smith et al., 2007). PL spectroscopy can help distinguish tortoise shell from some of its imitators; however, the results can be ambiguous, and interpretation must be combined with other gemological techniques (Hainschwang and Leggio, 2006).

RECENT ADVANCEMENTS

PL Mapping. For decades, gemologists have been using Raman and PL spectroscopy to answer the questions “What is the gem?” and “What are the defects?” With the advent of PL mapping in the past decade, we have been able to answer another question: “Where are the defects?”

Raman and PL mapping, sometimes referred to as *hyperspectral imaging*, is a logical extension of the applications described above. These techniques enable spectra to be quickly and automatically collected from an area rather than from a single point (or having to manually move the sample to collect multiple spectra from it). Improvements in the necessary instrumentation, such as computer hardware for data processing, detector efficiencies, and higher-power excitation sources, have made this possible. Therefore, Raman and PL mapping have emerged as preferred methods for analyzing spatial differences. As the computerized microscope stage scans across a gem, thousands of spectra are rapidly collected. This allows gemologists and researchers to piece together a detailed picture showing the areas with high intensities (or concentrations) of optical features. The ability to collect Raman and PL data quickly and easily has permitted fundamental studies of spatial variations within a gem that were not possible just a few years earlier (e.g., Eaton-Magaña et al., 2021; Laidlaw et al., 2021; Lai et al., 2024a). The technique opens many opportunities to explore growth processes and different treatments, as well as wider applications such as determining geological provenance.

Natural growth processes can create pronounced spatial variations of defects across gemstones. For example, yellow to orange diamonds colored by the 480 nm band (Lai et al., 2024b) and pink diamonds colored by the 550 nm band (Eaton-Magaña et al., 2020) have pronounced spatial differences. PL mapping of these gems reveals the defects that correspond to the color zoning.

Corundum. When corundum crystals form at depth, concentrations of chromium and other trace elements vary throughout the crystal in response to geological conditions. These minute variations can be imaged and mapped using PL spectroscopy. The 694 nm luminescence band is related to chromium, with its intensity resulting from a complex interplay between chromium and other trace elements that quench (reduce) or sensitize (increase) the intensity of Cr³⁺ luminescence (Calvo del Castillo et al., 2009). The interactions between quenchers or sensitizers and chromium remain poorly understood due to the variety of trace element substitutions in natural corundum and the difficulty in interpreting their relationships. Complete characterization often requires growing specially doped synthetic corundum crystals to restrict the number of concurrent interactions, or it may involve complex calculations based on crystal field theory. Quantitative determinations of chromium and trace element concentrations in crystal domains require chemical analysis.

Regardless of the specifics of quenchers and sensitizers of chromium luminescence in corundum, PL mapping can be a useful technique for imaging differences in natural versus synthetic corundum, provided the chromium concentrations vary sufficiently within the synthetic crystal. While natural corundum may undergo chaotic and varied growth processes, synthetic corundum is grown under more predictable and consistent conditions that can form regular oscillatory bands or curved striations, often seen as curved color banding when viewed under the microscope with diffused light. If the curvature of these oscillatory bands is not clearly visible, it can be difficult to discriminate from natural corundum. Due to its growth mechanisms, natural corundum displays straight or angular oscillatory bands.

In natural corundum, PL mapping is an important tool for choosing locations of interest to analyze, as both sapphires and rubies can exhibit complex zonation and a range in chemistry through-

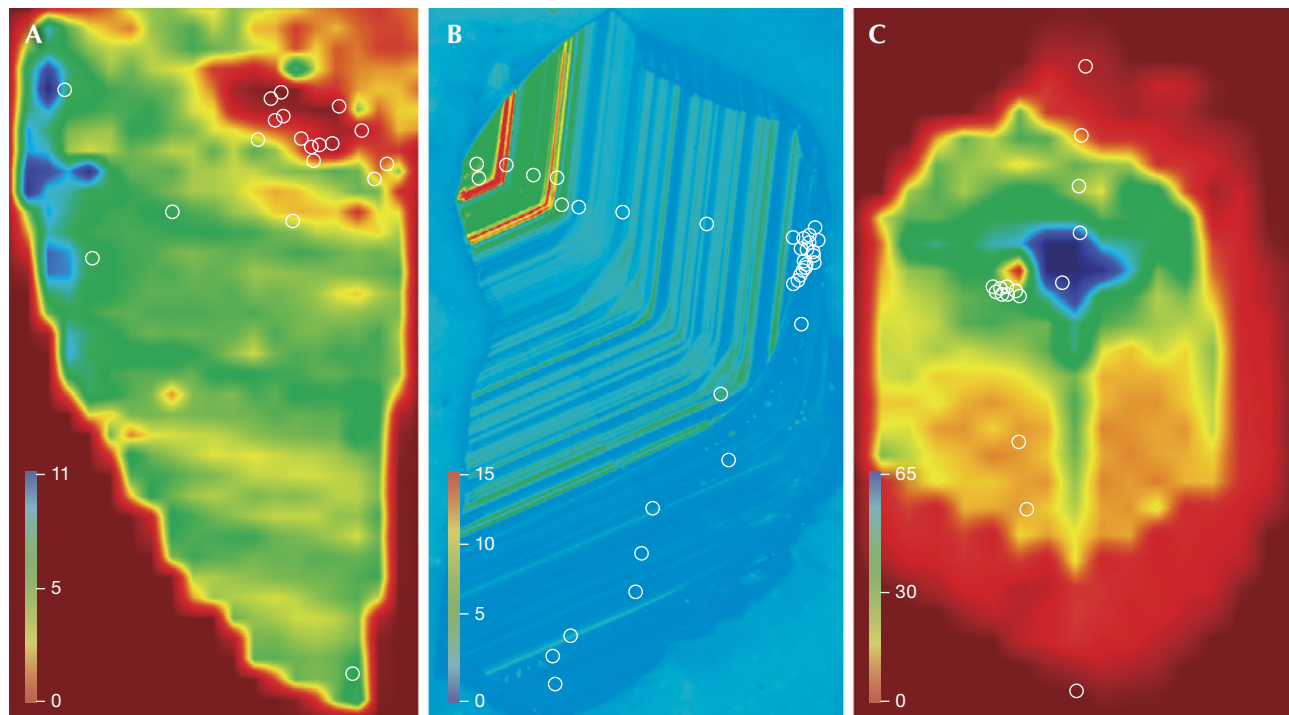
out the crystal (figure 8; Turnier, 2022). Zoning in natural corundum is more complex and varied than in synthetic corundum.

3D Mapping. Recent advances in technology and custom instruments have enabled the acquisition of high spectral and spatial resolution, large-volume three-dimensional measurements of gems (Jones et al., 2024a). While two-dimensional PL maps have demonstrated usefulness for a wide variety of gem applications (Eaton-Magaña et al., 2021; Laidlaw et al., 2021) and 2D depth profiling has also shown some promising applications (e.g., Lai et al., 2024b), those provide only a fraction of the available information about a gem. Full 3D spectroscopic imaging allows us to better understand a gemstone's growth history, distribution of defects, and the locations of inclusions. The speed of these systems is achieved through simultaneously collecting information along a line, as opposed to a point, which enables much more efficient 3D data collection.

High-resolution 3D PL mapping using a custom-built device at GIA has been successfully applied to natural and CVD-grown diamond. This technique has provided a wealth of information that was previously unattainable due to instrumentation issues or long collection times (Jones et al., 2024a). Shown in figure 9 are 2D PL images of a natural diamond, captured using 405 nm excitation. These false-color images contain a spectrum at each point, simplified to represent emission from three defects: N3 (blue), H3 (green), and plastic deformation-related features around 700 nm (red). Since data collection took place at room temperature, these spectra overlap. The relative concentrations vary across the sample, mixing to create colors such as yellow and orange, as shown in the core of figure 9A.

One of the challenges of PL mapping is how to best plot the results. Both samples in figure 9 are natural diamonds, cut in half and polished flat on one side. Sample A shows a colorless central region and a brown outer rim, with a different relative combi-

Figure 8. Representative false-color PL maps showing Cr³⁺-related luminescence in corundum. A: A Cambodian sapphire from Pailin Province with diffuse zoning (yellow and green colors). B: A Thai sample from Kanchanaburi with oscillatory growth zoning that decreases sharply with chromium content toward the rim. C: An Australian sapphire from Inverell shows diffuse core-to-rim zoning (perceived ridges at the yellow-red boundary are due to larger step size during PL mapping, which may also be related to the green linear features down the crystal center). The overlaid circles show the location of oxygen isotope analyses targeting different growth domains in the sapphires (Turnier, 2022).



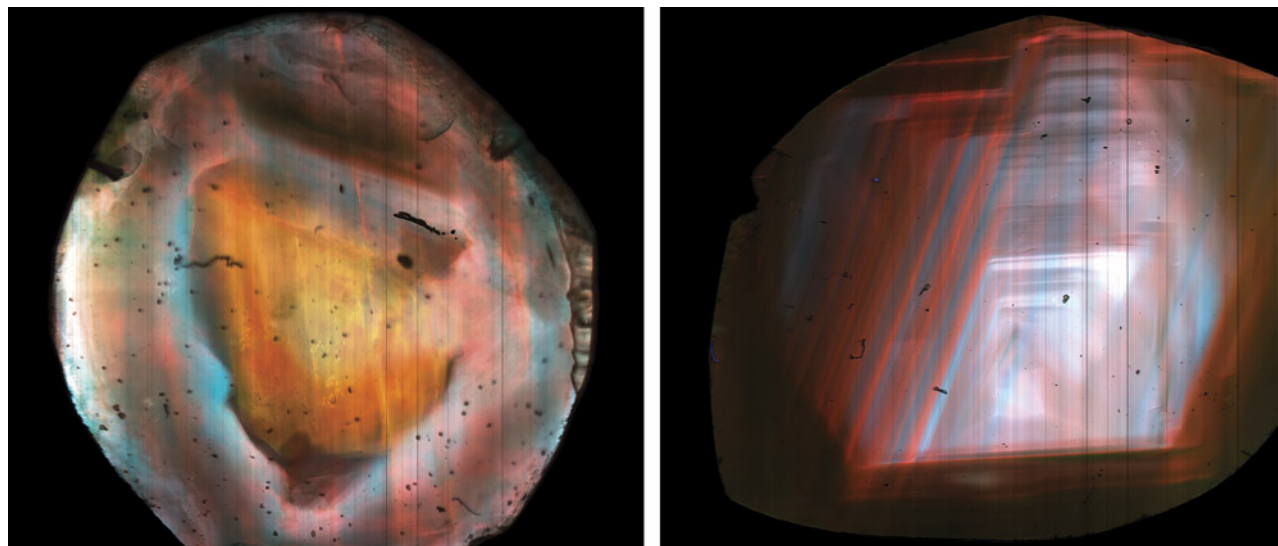


Figure 9. False-color images of two natural rough diamonds, cut in half with one polished face to show their internal growth structures. Broad sections of the spectra from each pixel were separated into blue (N3), green (H3), and red (plastic deformation-related luminescence at ~700 nm). Spectral overlap between features results in colors that represent combinations of defects. Sample A on the left is a natural diamond with two distinct growth phases: a colorless central core region and a brown-colored rim. Sample B on the right is a cross-section of natural diamond showing strong N3 emission with regions of higher H3 (appearing blue-green), with red lines representing plastic deformation throughout the growth structure. Both images are ~5.5 mm across and were acquired with a 4×0.16 NA objective lens using 405 nm excitation at room temperature. Images by Daniel Jones.

nation of the three defects. Sample B displays N3-related growth structure near the center of the stone, decreasing in intensity from core to rim. Both samples display plastic deformation-related emission in the red channel, which is sparser in A but follows the growth structure shown in B.

Figure 10 presents a subset of sample A using a 10×0.4 NA (numerical aperture) objective lens, imaged in 3D. Figure 10A shows cross-sectional images of scans along the XY, YZ, and XZ planes. The pink, red, and white areas indicate that the diamond actually experienced three growth events. The plastic deformation-related red emission penetrates in straight lines through the sample from core to rim. The two images shown in figure 10 (B and C) represent the full 3D dataset, which can be freely rotated and scanned at any angle to reveal the internal growth structure. Figure 10B represents the unsliced dataset, while figure 10C shows the same view but with a diagonal slice of the internal structure. This technique can be applied to determining the orientation of samples by identifying features related to specific growth directions. This helps researchers determine growth history to better understand the incorporation of inclusions during natural growth.

Large Databases and Statistics. Gemological laboratories are uniquely positioned to identify large-scale spectral trends from thousands of gemstones. Statistical analysis has been used for PL spectral data and other gem-related applications, including trace element data (e.g., Zhang et al., 2019; Chankhantha et al., 2020). Full use of the information requires automatic software processing to identify and analyze the spectral peaks and incorporate them into a searchable database. Statistical analysis can include factors such as the presence or absence of particular peaks across all selected lasers, the peak areas normalized to the diamond Raman line, and the peak widths. The data can be cross-referenced against color, diamond type, or concluded origin. Developing robust peak-finding and peak-matching algorithms for rapid automatic processing of all collected spectra is nearly as important as the analysis itself. Large-scale spectral data mining also has the potential to reveal new patterns among detected PL features and uncover previously hidden trends and relationships. For example, Hardman et al. (2022a) examined PL spectral differences in more than 2,000 natural green diamonds, correlating the normalized peak intensities with the presence of green and brown radiation

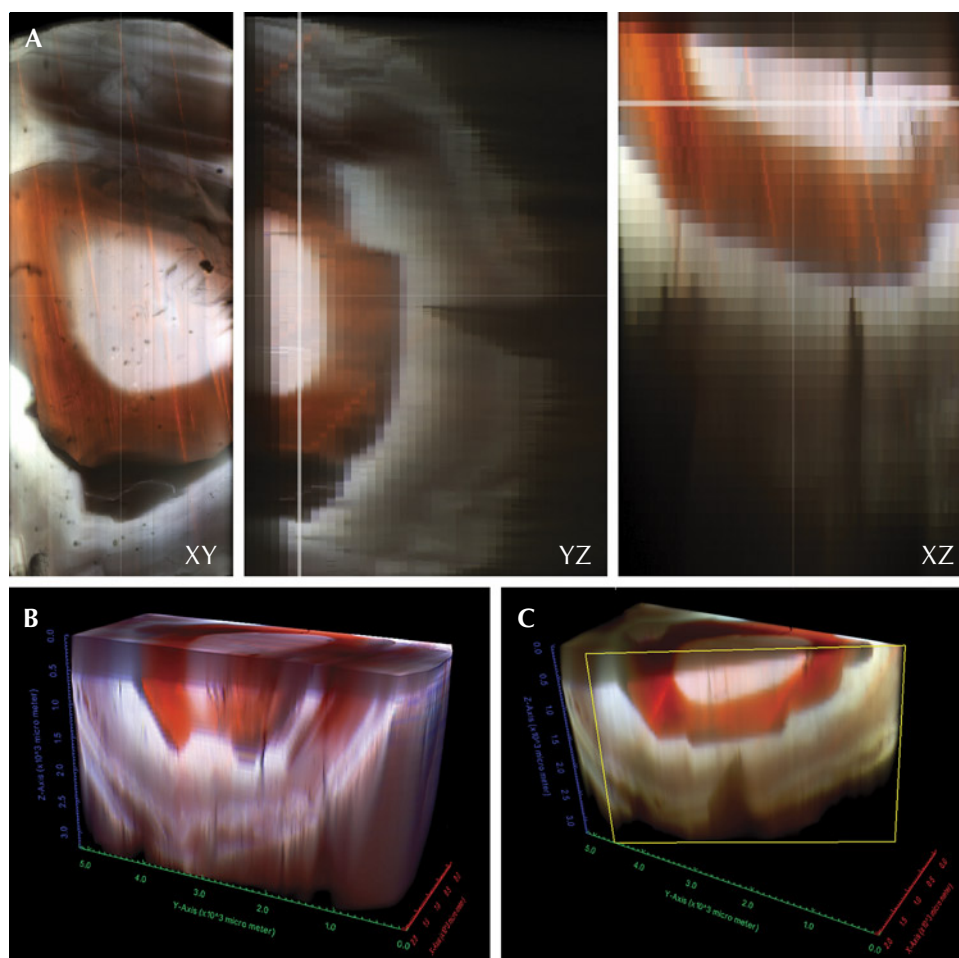


Figure 10. 3D representations of spectra for sample A from figure 9 (left), acquired with 405 nm excitation at room temperature. The spectra associated with each pixel were separated by wavelengths into blue (N3; ZPL = 415.2 nm), green (H3; ZPL = 503.2 nm), and red (plastic deformation-related luminescence at ~700 nm). A: These three images show XY, YZ, and XZ scans of the 3D data cube, indicating three growth events—a central core, another growth rim, and then an outer layer. B and C: Volumetric slices from the full 3D dataset, which can be selectively scanned and freely rotated. Image B is a visualization of the full dataset, while image C shows a diagonal slice through the dataset.

stains. Hardman et al. (2022b) examined the PL spectra of more than 11,000 CVD-grown diamonds to locate statistically significant peak differences between as-grown and HPHT-treated CVD-grown diamonds.

Although the specific details of datasets or computed models may be proprietary, the results can reveal previously unknown links between PL spectral features or between PL features and characteristics such as color or growth history (Hardman et al., 2024). However, machine learning and artificial intelligence methods should be seen as a tool to aid in research or gemological assessment. Statistical analysis should not be considered a replacement for expert judgment and experience that draws upon data from numerous tests and microscopic observations.

Time-Resolved Luminescence. Luminescence from defects does not occur instantaneously—it takes time for the electron to decay from the excited state back to the ground state, either emitting a photon of light or non-radiatively decaying. Broadly, we can

consider two types of luminescence: fluorescence and phosphorescence. This is a slight simplification, as there are additional complexities. Fluorescence occurs on pico- and nanosecond timescales, making it very fast and difficult to measure. Phosphorescence generally occurs on longer timescales, milliseconds or longer, and can be caused by several mechanisms within gemstones. Phosphorescence has been measured extensively both for diamond and other colored stones (McGuinness et al., 2020; Zhang and Shen, 2023). The time-domain intensity graphs generated from lifetime data are referred to as a “decay.”

Fluorescence is much more difficult to measure, but there are a few methods for measuring on these very fast timescales. Time-resolved luminescence, though not used regularly in gemstone analysis, has been implemented in a few applications (e.g., Liaugaudas et al., 2009, 2012; Monticone et al., 2013; Fisher, 2018; Dupuy and Phillips, 2019; Jones et al., 2019, 2021; McGuinness et al., 2020). The two techniques described here require the use of a pulsed laser, which

emits laser light in pulses less than ~1 nanosecond in duration. The “gold standard” is time-correlated single photon counting (TCSPC), which measures the arrival time of a single photon relative to the triggered pulses from the laser source. This method is slow, limited to a collection rate <5% of the repetition rate of the laser. The second method is time-gated measurement, where temporal gates are rapidly opened and closed to allow light from the emission to be detected. These gates are then moved through time in small increments to measure the full decay.

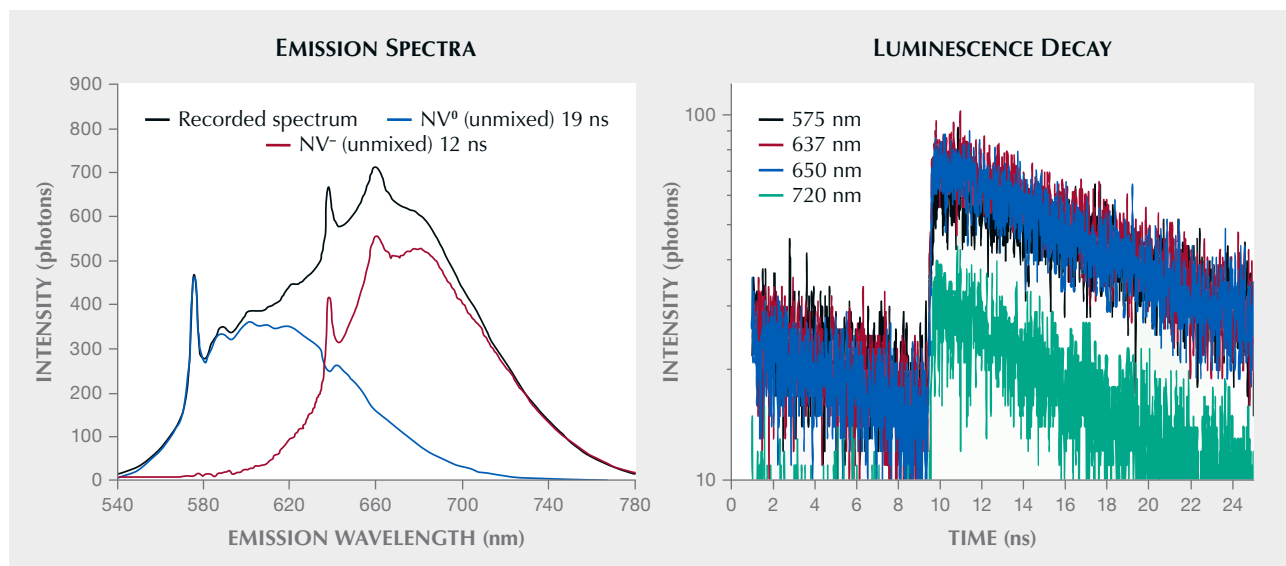
Data from these decays is typically modeled using an exponential decay model. Most single-defect species emit with a single lifetime, producing a monoexponential decay. When two or more defects overlap in the detection, or if quenching occurs, the decay will be more complex. In these cases, the different components can be fitted by a series of exponentials. Quenching occurs when energy is transferred from a donor defect to a nearby acceptor defect, reducing the emitting light and also the lifetime. A prime example is the interaction between N3 and A-center defects in diamond. The lifetime of N3 will decrease with increasing A-center concentrations, reducing the intensity of the light emitted from N3. This is an interesting mechanism because A-centers are best detected and quantified through

IR absorption, which means it may be possible to use the lifetime of the N3 center to measure the concentration of A-centers.

Examining the decay curves of various defects can reveal significant differences between nominally similar gems such as natural and treated diamonds. Ongoing research is investigating the differences in the decay times of various color centers between natural, treated, and laboratory-grown stones to extend beyond standard PL measurements (e.g., Eaton-Magaña, 2015). Each defect has a different characteristic lifetime, which can be used to separate them, and collecting lifetime data per wavelength can reveal the spectra for overlapping components. Lifetime measurements with short timescales require more specialized lab equipment including fast detectors and electronics, pulsed lasers, and spectral blocking mechanisms such as spectrometers and filters. An alternative method for analyzing lifetime data comes from mathematical transformations of the decay data in a phasor plot. More detailed information on its application to gemstones can be found in Jones et al. (2021).

Figure 11 (left) shows data from a CVD-grown diamond containing NV⁰ and NV⁻, acquired through TCSPC using a 510 nm excitation source. The collected spectrum (generated from the sum of all photons in the decay) is shown in figure 11 (left), and this

Figure 11. A CVD-grown diamond containing both NV charge states was measured using TCSPC with 510 nm excitation, and the sample’s luminescence decay was measured every 1 nm for the wavelength range of 540–780 nm (left). Right: Examples of the decays are shown, fitted with a double exponential decay function yielding decay times of 19 ns for NV⁰ and 12 ns for NV⁻.



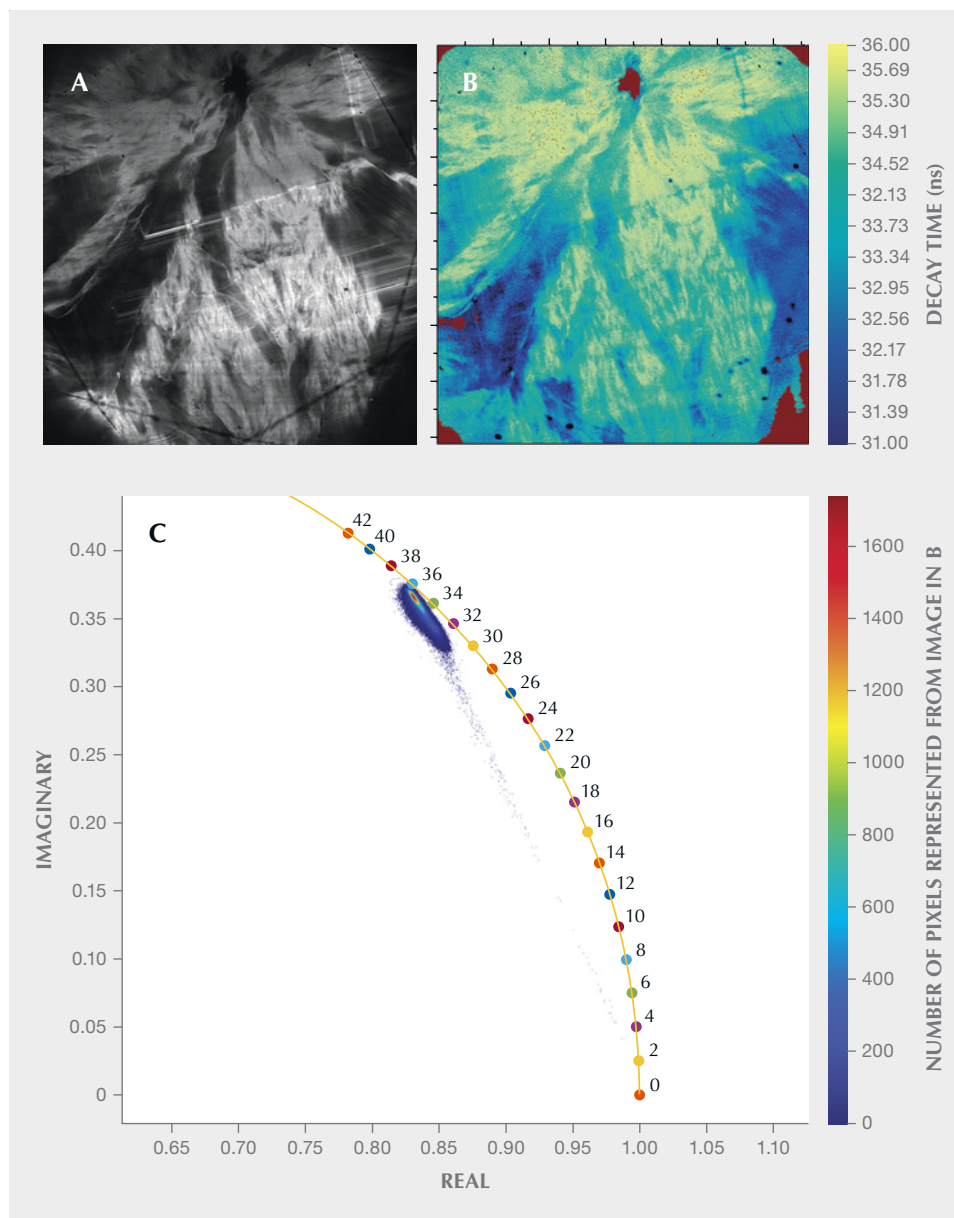


Figure 12. A: The summed intensity image of a natural brown diamond shows unusual cloud-like networks acquired from TCSPC lifetime data using 405 nm excitation. B: The same region of the sample is shown, but with the phase lifetime extracted through phasor analysis of the decays present at each pixel. C: A phasor plot of image B shows decay times (in nanoseconds) along the circumference of a section of a circle, called the universal circle; see Jones et al., 2021). The color bar represents the pixels from image B located at that point in the histogram. The data is clustered near the 35 ns data-point, indicating the predominant decay time.

represents something that can be acquired conventionally. Decays at four wavelengths are shown in figure 11 (right), displaying a subtle variation in the decay. By fitting a double exponential decay model with time constants of 12 and 19 ns, representing NV^- and NV^0 , respectively, the two NV spectra can be unmixed from the recorded spectrum (shown in blue and red). This demonstrates that lifetime can be used to separate overlapping spectral features. The fitted lifetimes agree well with those determined on these two centers individually: 13 ± 0.5 ns for NV^0 (Collins et al., 1983a) and 19 ± 2 ns for NV^- (Liaugaudas et al., 2012).

Factors affecting emission are the impurities' valence state, structure, charge, and the appearance of other impurities (Gaft and Panczer, 2013). Previous studies on diamond have shown that the decay time can be reduced by quenching, in which energy transfers to other impurities. This can create several distinct observed lifetimes for an optical center. For example, the intrinsic lifetime of NV^0 (ZPL at 575.0 nm) in high-purity, low-nitrogen samples is given as 19 ± 2 ns (Liaugaudas et al., 2012). However, quenching of the single substitutional nitrogen (N_s^0) can shorten the NV^0 lifetime (Monticone et al., 2013). Therefore, HPHT treatment of diamond can help

shorten the decay time of NV⁰ centers by increasing the concentration of N_s⁰ (although other factors can complicate the analysis). While many diamond-related defects have been shown to have short decay times on nanosecond timescales, some researchers have shown that other defects yet to be characterized exist for a longer duration, from microseconds to milliseconds, and can also be useful for gemstone identification (Eaton-Magaña et al., 2008; Fisher, 2018).

As mentioned above, PL mapping involves collecting thousands of spectra across a sample's surface. The same can be accomplished for lifetime data in a method called fluorescence lifetime imaging microscopy (FLIM). Lifetime images are shown in figure 12 for a diamond and in figure 13 for a sapphire and emerald. These maps take longer to acquire than PL maps due to the large number of photons needed for a good data fit, which is necessary for accurate lifetime measurement. It is also highly beneficial to detect light only over a narrow, well-selected wavelength range for measuring the lifetime of a single emitter.

The authors measured the N3 lifetime of a natural faceted diamond using 405 nm excitation with 5 μm pixels. The intensity image shown in figure 12A reveals a network of filaments in a cloud-like structure, extending from a core near the top of the image, with bright lines crossing through filaments that resemble standard growth structure. The lifetime map in figure 12B shows a scale from 36 to 31 ns (where the natural lifetime of N3 is reported to be 41 ns; Thomaz and Davies, 1978), which could indicate the presence of A-centers. This map shows that the lower-intensity regions have a shorter lifetime, and the phasor plot in figure 12C indicates that most of the pixels are clustered around 35 ns. Lifetime measurements are very sensitive to weak emission, and even a low concentration of a very different lifetime component can show contrast.

While diamond is often the focus of research on luminescence decay times, studies have also been conducted on other gemstones. Naturally irradiated fluorite exhibits red photoluminescence at 750 and 635 nm with decay times of 20.3 and <5 ns, respec-

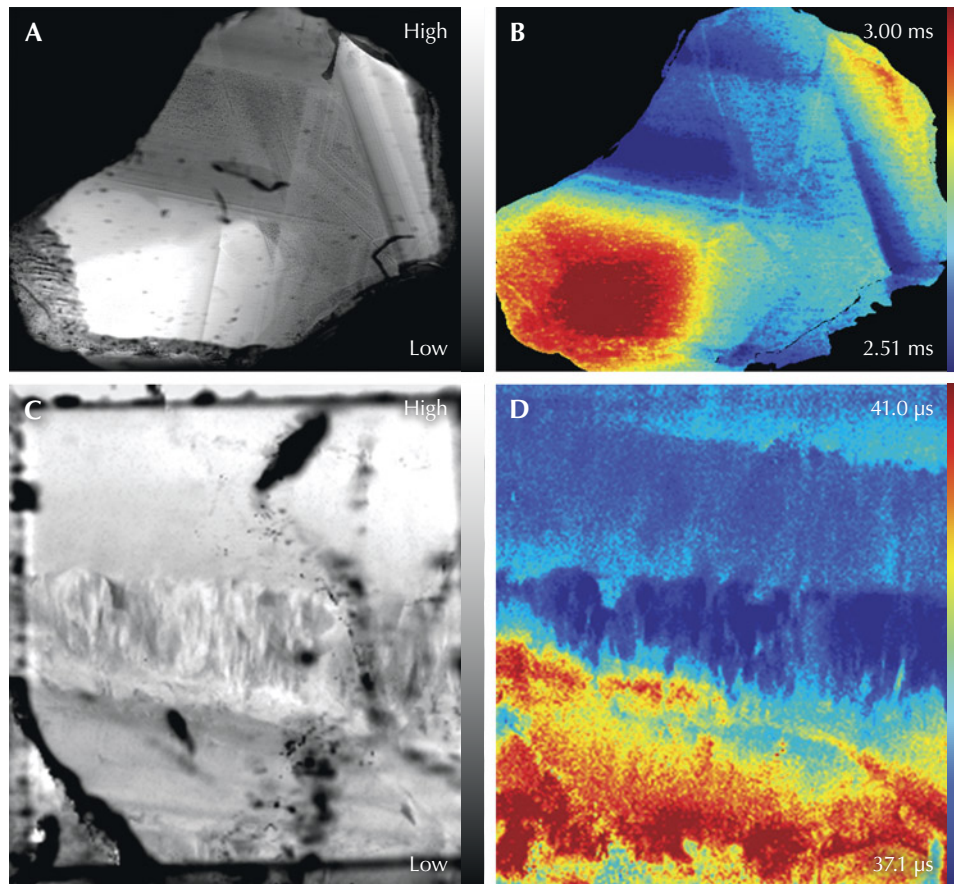


Figure 13. Images A and B show a natural blue sapphire plate measured with TCSPC using 405 nm excitation and detecting the emission band of Cr³⁺, where A shows the summed intensity and B the weighted mean lifetime. Growth structure is apparent in both images. C and D show a faceted untreated emerald measured using 405 nm excitation with emission centered at 684 nm, where C shows the summed intensity and D the weighted mean lifetime. The summed intensity map is heavily affected by the inclusions and cracks in the sample, but the lifetime map is resistant to these features, revealing various growth structures. Fields of view 6.5 mm (A) and 3.1 mm (C).

tively (Gaft et al., 2020). The photoluminescence features of spinel and alexandrite, with lifetimes on the microsecond timescale, can be more readily detected and chronicled than defects with nanosecond lifetimes. Xu et al. (2023) determined the lifetime for the chromium peak at 685–687 nm as 9–23 μ s in spinel and 25–53 μ s in alexandrite. Although there was some overlap in lifetimes, the researchers were able to distinguish natural, treated, and laboratory-grown spinel, as well as natural and laboratory-grown alexandrite.

One of the more widely studied lifetimes in gemstones other than diamond is that of Cr^{3+} . In the past, this was because of its viability for a laser gain medium, where lifetime is an important factor, such as ruby. The natural lifetime of Cr^{3+} is 3.43 ms, though this can be reduced by various other defects (Seat and Sharp, 2004; Jones et al., 2024b). Figure 13 (A and B) shows a natural blue sapphire plate measured with TCSPC using 405 nm excitation. The emission was centered on the double Cr^{3+} peaks at 692.8 (R1) and 694.2 nm (R2), and the summed intensity image in figure 13A indicates growth structure. The lifetime map in figure 13B shows very different lifetimes over the sample, indicating the presence of different unknown quenching species.

An untreated faceted emerald was also measured using 405 nm excitation, with an emission band cen-

tered at 684 nm. The literature (e.g., Xu et al., 2023) suggests that this is Cr^{3+} , but it possesses a much shorter decay time than chromium in corundum. While the intensity map in figure 13C shows many cracks and inclusions, the lifetime map in figure 13D clearly shows growth structure, with a small variation in lifetime. The clarity of the features shown in the lifetime map contrasts with the large changes in intensity caused by cracks and inclusions, demonstrating one of the advantages of lifetime measurements over intensity maps: their resistance to these types of clarity features.

Time-resolved luminescence has proven useful in resolving PL bands that overlap with very intense luminescence from Cr^{3+} , which has a long decay time of 3.43 ms (Chandler et al., 2006), as well as other PL bands that typically have much shorter lifetimes compared to chromium luminescence.

CONCLUSIONS

As a nondestructive tool, PL spectroscopy is vital in many ways: identifying gemstones, evaluating the origin of their color, and occasionally providing clues about their geographic origin. As treatments become more prevalent and sophisticated, gemologists must look for increasingly subtle clues to distinguish nat-

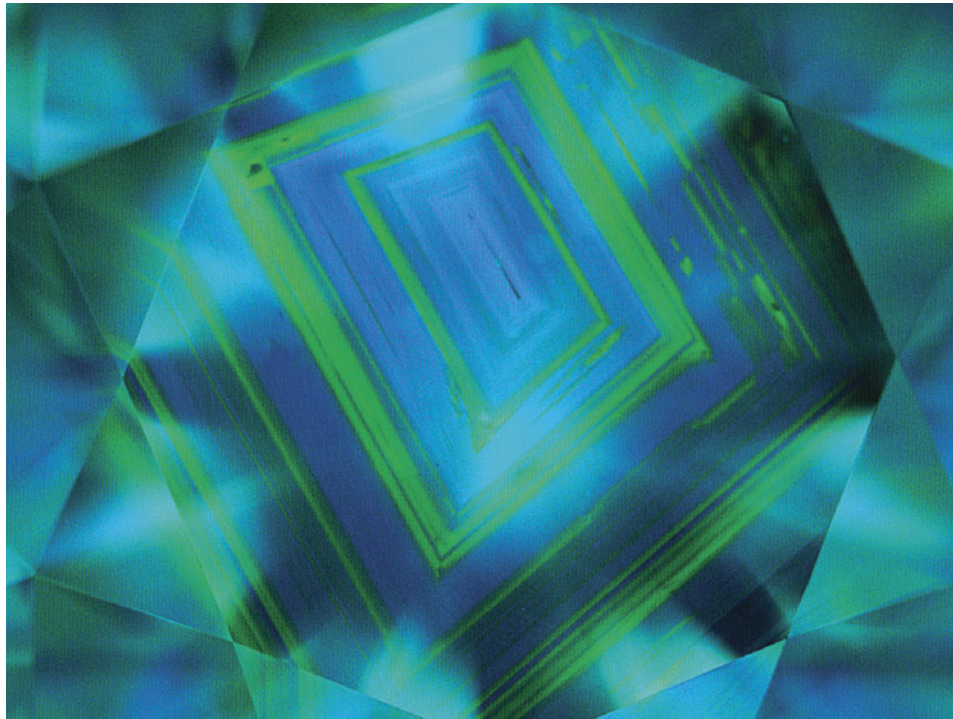


Figure 14. Natural type Ia diamonds often show a growth pattern that has been compared to the growth rings of a tree. However, it is not as common to see the alternating pattern of blue fluorescence (due to the N3 center) and green (due to H3/H4 centers) shown in this 1.83 ct K-color diamond with SI₂ clarity. PL spectroscopy is very useful for confirming these centers and for detecting much weaker optical centers. Image by GIA staff.

ural from laboratory-grown gemstones and untreated from treated gemstones. Therefore, many gemstones are subjected to several types of spectroscopy to reveal histories hidden in defects that occur in very low concentrations.

In recent decades, as the use of PL spectroscopy has become more common in gemological research laboratories, PL analysis itself has become more sophisticated. Every gem, whether natural, laboratory-

grown, or treated in some manner, has its own story (e.g., figure 14), and every consumer can learn their gem's story through proper identification. Over the past 25 years, PL analysis has become a powerful, highly sensitive research tool leading to many recent discoveries about diamond and other gemstones, revealing subtle distinctions that can significantly affect commercial value. This helps to ensure public confidence in the gem and jewelry industry.

ABOUT THE AUTHORS

Dr. Sally Eaton-Magaña is senior manager of diamond identification, Dr. Rachelle Turnier is GIA Museum manager, and Dr. Christopher M. Breeding is senior manager of analytics, at GIA in Carlsbad, California. Dr. Daniel Jones is a research scientist at GIA in New Jersey.

ACKNOWLEDGMENTS

The authors would like to thank Andy Shen for his help in collecting the photoluminescence spectra shown in figure 4, which

were collected while he was at GIA, and Artitaya Homkrajae (GIA, Carlsbad) for her very helpful suggestions. We also express our gratitude to Adrian Chan (GIA, New Jersey) for cutting and polishing the two natural diamond samples and Aaron Palke (GIA, Carlsbad) for providing the sapphire and emerald plates. We sincerely thank Paul French, Chris Dunsby, Daan Arroo, and Neil Alford (Imperial College London) for providing the sample and equipment for the lifetime measurements of the NV-containing CVD diamond.

REFERENCES

- Ashfold M.N.R., Goss J.P., Green B.L., May P.W., Newton M.E., Peaker C.V. (2020) Nitrogen in diamond. *Chemical Reviews*, Vol. 120, No. 12, pp. 5745–5794, <http://dx.doi.org/10.1021/acs.chemrev.9b00518>
- Bakhtin A.I., Denisov I.G., Lopatin O.N. (1995) Photoluminescence of hole centers in olivine crystals. *Optics and Spectroscopy*, Vol. 79, No. 5, pp. 773–777.
- Berry R.F., Danyushevsky L.V., Goemann K., Parbhakar-Fox A., Rodemann T. (2017) Micro-analytical technologies for mineral mapping and trace element deportment. In B.G. Lottermoser, Ed., *Environmental Indicators in Metal Mining*, Springer, Switzerland, pp. 55–72.
- Bersani D., Lottici P.P. (2010) Applications of Raman spectroscopy to gemology. *Analytical and Bioanalytical Chemistry*. Vol. 397, No. 7, pp. 2631–2646, <http://dx.doi.org/10.1007/s00216-010-3700-1>
- Breeding C.M., Shen A.H., Eaton-Magaña S., Rossman G.R., Shigley J.E., Gilbertson A. (2010) Developments in gemstone analysis techniques and instrumentation during the 2000s. *G&G*, Vol. 46, No. 3, pp. 241–257, <http://dx.doi.org/10.5741/GEMS.46.3.241>
- Calderon T., Millan A., Jaque F., Solé J.G. (1990) Optical properties of Sm²⁺ and Eu²⁺ in natural fluorite crystals. *International Journal of Radiation Applications and Instrumentation. Part D. Nuclear Tracks and Radiation Measurements*, Vol. 17, No. 4, pp. 557–561, [http://dx.doi.org/10.1016/1359-0189\(90\)90016-Q](http://dx.doi.org/10.1016/1359-0189(90)90016-Q)
- Calderon T., Khanlary M.-R., Rendell H.M., Townsend P.D. (1992) Luminescence from natural fluorite crystals. *International Journal of Radiation Applications and Instrumentation. Part D. Nuclear Tracks and Radiation Measurements*, Vol. 20, No. 3, pp. 475–485, [http://dx.doi.org/10.1016/1359-0189\(92\)90033-R](http://dx.doi.org/10.1016/1359-0189(92)90033-R)
- Calvo del Castillo H., Deprez N., Dupuis T., Mathis F., Deneckere A., Vandenaebale P., Calderón T., Strivay D. (2009) Towards the differentiation of non-treated and treated corundum minerals by ion-beam-induced luminescence and other complementary techniques. *Analytical and Bioanalytical Chemistry*, Vol. 394, No. 4, pp. 1043–1058, <http://dx.doi.org/10.1007/s00216-009-2679-y>
- Chalain J.-P., Fritsch E., Hänni H.A. (2000) Identification of GE POL diamonds: A second step. *Journal of Gemmology*, Vol. 27, No. 2, pp. 73–78.
- Chandler D.E., Majumdar Z.K., Heiss G.J., Clegg R.M. (2006) Ruby crystal for demonstrating time- and frequency-domain methods of fluorescence lifetime measurements. *Journal of Fluorescence*, Vol. 16, No. 6, pp. 793–807, <http://dx.doi.org/10.1007/s10895-006-0123-7>
- Chankhantha C., Amphon R., Rehman H.U., Shen A.H. (2020) Characterisation of pink-to-red spinel from four important localities. *Journal of Gemmology*, Vol. 37, No. 4, pp. 393–403.
- Chen Y., Zheng J., Lu M., Liu Z., Zhou Z. (2024) Gemological and spectral characteristics of gem-quality blue gahnite from Nigeria. *Journal of Spectroscopy*, article no. 6693346, <http://dx.doi.org/10.1155/2024/6693346>
- Clark C.D., Norris C.A. (1971) Photoluminescence associated with the 1.673, 1.944 and 2.498 eV centres in diamond. *Journal of Physics C: Solid State Physics*, Vol. 4, No. 14, pp. 2223–2229, <http://dx.doi.org/10.1088/0022-3719/4/14/036>
- Collins A.T. (1992) The characterisation of point defects in diamond by luminescence spectroscopy. *Diamond and Related Materials*, Vol. 1, No. 5-6, pp. 457–469, [http://dx.doi.org/10.1016/0925-9635\(92\)90146-F](http://dx.doi.org/10.1016/0925-9635(92)90146-F)
- Collins A.T., Thomaz M.F., Jorge M.I.B. (1983a) Luminescence decay time of the 1.945 eV centre in type Ib diamond. *Journal of Physics C: Solid State Physics*, Vol. 16, No. 11, pp. 2177–2181, <http://dx.doi.org/10.1088/0022-3719/16/11/020>
- Collins A.T., Thomaz M.F., Jorge M.I.B. (1983b) Excitation and decay of H4 luminescence in diamond. *Journal of Physics C:*

- Solid State Physics*, Vol. 16, No. 28, pp. 5417–5425, <http://dx.doi.org/10.1088/0022-3719/16/28/009>
- Culka A., Hyršl J., Jehlička J. (2016) Gem and mineral identification using GL gem Raman and comparison with other portable instruments. *Applied Physics A*, Vol. 122, No. 11, article no. 959, <http://dx.doi.org/10.1007/s00339-016-0500-2>
- Deeva V.A., Shelementiev Y.B. (2002) Gemological properties of synthetic flux spinel. *Gemmological Bulletin*, No. 6, pp. 9–17.
- D'Haenens-Johansson U.F.S., Butler J.E., Katrusha A.N. (2022) Synthesis of diamonds and their identification. *Reviews in Mineralogy and Geochemistry*, Vol. 88, No. 1, pp. 689–753, <http://dx.doi.org/10.2138/rmg.2022.88.13>
- Dupuy H., Phillips J.C. (2019) Selecting a diamond verification instrument based on the results of the Assure Program: An initial analysis. *Journal of Gemmology*, Vol. 36, No. 7, pp. 606–619.
- Eaton-Magaña S. (2015) Comparison of luminescence lifetimes from natural and laboratory irradiated diamonds. *Diamond and Related Materials*, Vol. 58, pp. 94–102, <http://dx.doi.org/10.1016/j.diamond.2015.06.007>
- Eaton-Magaña S., Ardon T. (2016) Temperature effects on luminescence centers in natural type IIb diamonds. *Diamond and Related Materials*, Vol. 69, pp. 86–95, <http://dx.doi.org/10.1016/j.diamond.2016.07.002>
- Eaton-Magaña S., Breeding C.M. (2016) An introduction to photoluminescence spectroscopy for diamond and its application in gemology. *G&G*, Vol. 52, No. 1, pp. 2–17, <http://dx.doi.org/10.5741/GEMS.52.1.2>
- Eaton-Magaña S.C., Shigley J.E. (2016) Observations on CVD-grown synthetic diamonds: A review. *G&G*, Vol. 52, No. 3, pp. 222–245, <http://dx.doi.org/10.5741/GEMS.52.3.222>
- Eaton-Magaña S., Post J.E., Heaney P.J., Freitas J., Klein P., Walters R., Butler J.E. (2008) Using phosphorescence as a fingerprint for the Hope and other blue diamonds. *Geology*, Vol. 36, No. 1, pp. 83–86, <http://dx.doi.org/10.1130/G24170A.1>
- Eaton-Magaña S.C., Shigley J.E., Breeding C.M. (2017) Observations on HPHT-grown synthetic diamonds: A review. *G&G*, Vol. 53, No. 3, pp. 262–284, <http://dx.doi.org/10.5741/GEMS.53.3.262>
- Eaton-Magaña S., McElhenny G., Breeding C.M., Ardon T. (2020) Comparison of gemological and spectroscopic features in type IIa and Ia natural pink diamonds. *Diamond and Related Materials*, Vol. 105, article no. 107784, <http://dx.doi.org/10.1016/j.diamond.2020.107784>
- Eaton-Magaña S., Breeding C.M., Palke A.C., Homkrajae A., Sun Z., McElhenny G. (2021) Raman and photoluminescence mapping of gem materials. *Minerals*, Vol. 11, No. 2, article no. 177, <http://dx.doi.org/10.3390/min11020177>
- Fiquet G., Richet P., Montagnac G. (1999) High-temperature thermal expansion of lime, periclase, corundum and spinel. *Physics and Chemistry of Minerals*, Vol. 27, pp. 103–111, <http://dx.doi.org/10.1007/s002690050246>
- Fisher D. (2018) Addressing the challenges of detecting synthetic diamonds. *G&G*, Vol. 54, No. 3, pp. 263–264.
- Fisher D., Spits R.A. (2000) Spectroscopic evidence of GE POL HPHT-treated natural type IIa diamonds. *G&G*, Vol. 36, No. 1, pp. 42–49, <http://dx.doi.org/10.5741/GEMS.36.1.42>
- Freitas J.A. Jr., Klein P.B., Collins A.T. (1994) Evidence of donor-acceptor pair recombination from a new emission band in semiconducting diamond. *Applied Physics Letters*, Vol. 64, No. 16, pp. 2136–2138, <http://dx.doi.org/10.1063/1.111710>
- Fritsch E., Massuyeau F., Rondeau B., Segura O., Hainschwang T. (2011) Advancing the understanding of luminescence in gem materials. *G&G*, Vol. 47, No. 2, p. 123.
- Gaft M., Panczer G. (2013) Laser-induced time-resolved luminescence spectroscopy of minerals: A powerful tool for studying the nature of emission centres. *Mineralogy and Petrology*, Vol. 107, No. 3, pp. 363–372, <http://dx.doi.org/10.1007/s00710-013-0293-3>
- Gaft M., Reisfeld R., Panczer G. (2015) *Modern Luminescence Spectroscopy of Minerals and Materials*. Springer International Publishing, Berlin, 606 pp.
- Gaft M., Waychunas G.A., Rossman G.R., Nagli L., Panczer G., Cheskis D., Raichlin Y. (2020) Red photoluminescence and purple color of naturally irradiated fluorite. *Physics and Chemistry of Minerals*, Vol. 47, No. 11, article no. 46, <http://dx.doi.org/10.1007/s00269-020-01116-4>
- García-Toloza J., Herreño-Daza M.J., González-Durán A.F., Cedeño-Ochoa C.J., Angarita-Sarmiento L.G. (2019) Photoluminescence analysis to determine the origin of emeralds from the Eastern and Western belts in Colombia. In *Proceedings of the 15th Biennial Meeting SGA, Glasgow, Scotland*, Vol. 2, pp. 931–934.
- Glynn T.J., Imbusch G.F., Walker G. (1991) Luminescence from Cr³⁺ centres in forsterite (Mg₂SiO₄). *Journal of Luminescence*, Vol. 48–49, pp. 541–544, [http://dx.doi.org/10.1016/0022-2313\(91\)90188-2](http://dx.doi.org/10.1016/0022-2313(91)90188-2)
- Green B. (2013) Optical and magnetic resonance studies of point defects in single crystal diamond. PhD thesis, University of Warwick, UK.
- Green B.L., Collins A.T., Breeding C.M. (2022) Diamond spectroscopy, defect centers, color, and treatments. *Reviews in Mineralogy and Geochemistry*, Vol. 88, No. 1, pp. 637–688, <http://dx.doi.org/10.2138/rmg.2022.88.12>
- Groat L.A., Giuliani G., Stone-Sundberg J., Sun Z., Renfro N.D., Palke A.C. (2019) A review of analytical methods used in geographic origin determination of gemstones. *G&G*, Vol. 55, No. 4, pp. 512–535, <http://dx.doi.org/10.5741/GEMS.55.4.512>
- Gugushev C., Götz J., Göbbels M. (2010) Cathodoluminescence microscopy and spectroscopy of synthetic ruby crystals grown by the optical floating zone technique. *American Mineralogist*, Vol. 95, No. 4, pp. 449–455, <http://dx.doi.org/10.2138/am.2010.3291>
- Hainschwang T., Leggio L. (2006) The characterization of tortoise shell and its imitations. *G&G*, Vol. 42, No. 1, pp. 36–52, <http://dx.doi.org/10.5741/GEMS.42.1.36>
- Hainschwang T., Fritsch E., Gaillou E., Shen A. (2024) Analysing the luminescence of gems. *Elements*, Vol. 20, No. 5, pp. 312–317, <http://dx.doi.org/10.2138/gselements.20.5.312>
- Hardman M.F., Eaton-Magaña S., Breeding C.M., Bassoo R. (2022a) Evaluating the effects of natural radiation exposure on green diamonds. Presented at the 2022 Goldschmidt Conference, Honolulu, <http://dx.doi.org/10.46427/gold2022.13133>
- Hardman M.F., Eaton-Magaña S.C., Breeding C.M., Ardon T., D'Haenens-Johansson U.F.S. (2022b) Evaluating the defects in CVD diamonds: A statistical approach to spectroscopy. *Diamond and Related Materials*, Vol. 130, article no. 109508, <http://dx.doi.org/10.1016/j.diamond.2022.109508>
- Hardman M.F., Homkrajae A., Eaton-Magaña S., Breeding C.M., Palke A.C., Sun Z. (2024) Classification of gem materials using machine learning. *G&G*, Vol. 60, No. 3, pp. 306–329, <http://dx.doi.org/10.5741/GEMS.60.3.306>
- Hughes R.W., Manorotkul W., Hughes E.B. (2017) *Ruby & Sapphire: A Gemologist's Guide*. RWH Publishing, Bangkok, 733 pp.
- Iakubovskii K., Adriaenssens G.J., Vohra Y.K. (2001) Nitrogen incorporation in CVD diamond. *Diamond and Related Materials*, Vol. 10, No. 3–7, pp. 485–489, [http://dx.doi.org/10.1016/S0925-9635\(00\)00436-2](http://dx.doi.org/10.1016/S0925-9635(00)00436-2)
- Ivakin U.D., Danchevskaya M.N., Muravieva G.P., Ovchinnikova O.G. (2003) Physicochemical properties of corundum doped in supercritical water. *High Pressure Science and Technology*, Joint 19th AIRAPT and 41st EHPRG Conference, Bordeaux.
- Iwahashi Y., Akamatsu S. (1994) Porphyrin pigment in black-lip pearls and its application to pearl identification. *Fisheries Science*, Vol. 60, No. 1, pp. 69–71, <http://dx.doi.org/10.2331/fishsci.60.69>
- Jin S., Smith E.M. (2024) Raman spectroscopy and X-ray diffraction in gemology: Identifying mineral species and other phases. *G&G*, Vol. 60, No. 4, pp. 518–535, <http://dx.doi.org/10.5741/GEMS.60.4.518>

- Johnson P., Moe K.S., Persaud S., Odake S., Kazuchits N.M., Zaitsev A.M. (2023) Spectroscopic characterization of yellow gem quality CVD diamond. *Diamond and Related Materials*, Vol. 140, article no. 110505, <http://dx.doi.org/10.1016/j.diamond.2023.110505>
- Jones D.C., Kumar S., Lanigan P.M.P., McGuinness C.D., Dale M.W., Twitchen D.J., Fisher D., Martineau P.M., Neil M.A.A., Dunsby C., French P.M.W. (2019) Multidimensional luminescence microscope for imaging defect colour centres in diamond. *Methods and Applications in Fluorescence*, Vol. 8, No. 1, article no. 014004, <http://dx.doi.org/10.1088/2050-6120/ab4eac>
- Jones D.C., Alexandrov Y., Curry N., Kumar S., Lanigan P.M.P., McGuinness C.D., Dale M.W., Twitchen D.J., Fisher D., Neil M.A.A., Dunsby C., French P.M.W. (2021) Multidimensional spectroscopy and imaging of defects in synthetic diamond: Excitation-emission-lifetime luminescence measurements with multiexponential fitting and phasor analysis. *Journal of Physics D: Applied Physics*, Vol. 54, No. 4, article no. 045303, <http://dx.doi.org/10.1088/1361-6463/abbde2>
- Jones D.C., Jollands M.C., D'Haenens-Johansson U.F.S., Muchnikov A.B., Tsai T.H. (2024a) Development of a large volume line scanning, high spectral range and resolution 3D hyperspectral photoluminescence imaging microscope for diamond and other high refractive index materials. *Optics Express*, Vol. 32, No. 9, pp. 15231–15242, <http://dx.doi.org/10.1364/OE.516046>
- Jones D.C., Jollands M.C., Jin S., Stewart-Barry S.S., Dale M.W., Green B.L. (2024b) Resolving and imaging ultra-low H concentrations in partially protonated Mg:α Al₂O₃ using FRET and the luminescence lifetime of Cr³⁺. *Journal of Materials Chemistry C*, Vol. 12, No. 39, pp. 16004–16014, <http://dx.doi.org/10.1039/D4TC02646B>
- Karampelas S., Fritsch E., Mevellec J.-Y., Gauthier J.-P., Sklavounos S., Soldatos T. (2007) Determination by Raman scattering of the nature of pigments in cultured freshwater pearls from the mollusk *Hyriopsis cumingi*. *Journal of Raman Spectroscopy*, Vol. 38, No. 2, pp. 217–230, <http://dx.doi.org/10.1002/jrs.1626>
- Karampelas S., Fritsch E., Hainschwang T., Gauthier J.-P. (2011) Spectral differentiation of natural-color saltwater cultured pearls from *Pinctada margaritifera* and *Pteria sterna*. *G&G*, Vol. 47, No. 2, p. 117.
- Karampelas S., Fritsch E., Makhloof F., Mohamed F., Al-Alawi A. (2020) Raman spectroscopy of natural and cultured pearls and pearl producing mollusc shells. *Journal of Raman Spectroscopy*, Vol. 51, No. 9, pp. 1813–1821, <http://dx.doi.org/10.1002/jrs.5670>
- Kiefert L., Karampelas S. (2011) Use of the Raman spectrometer in gemmological laboratories: Review. *Spectrochimica Acta Part A: Molecular and Biomolecular Spectroscopy*, Vol. 80, No. 1, pp. 119–124, <http://dx.doi.org/10.1016/j.saa.2011.03.004>
- Kitawaki H., Okano M. (2006) Spinel up to date. GAAJ Research Lab Report, https://grjapan.ddo.jp/gaaj_report/2006/2006_03-01en.html
- Komarovskikh A., Rakhmanova M., Yuryeva O., Nadolniny V. (2020) Infrared, photoluminescence, and electron paramagnetic resonance characteristic features of diamonds from the Aikhal pipe (Yakutia). *Diamond and Related Materials*, Vol. 109, article no. 108045, <http://dx.doi.org/10.1016/j.diamond.2020.108045>
- Kondo D., Befi R., Beaton D. (2010) Lab Notes: Heat-treated spinel. *G&G*, Vol. 46, No. 2, pp. 145–146.
- Lai M.Y., Breeding C.M., Stachel T., Stern R.A. (2020) Spectroscopic features of natural and HPHT-treated yellow diamonds. *Diamond and Related Materials*, Vol. 101, article no. 107642, <http://dx.doi.org/10.1016/j.diamond.2019.107642>
- Lai M.Y., Hardman M.F., Eaton-Magaña S., Breeding C.M., Schwartz V.A., Collins A.T. (2024a) Spectroscopic characterization of diamonds colored by the 480 nm absorption band. *Diamond and Related Materials*, Vol. 142, article no. 110825, <http://dx.doi.org/10.1016/j.diamond.2024.110825>
- Lai M.Y., Myagkaya E., Hardman M.F., Eaton-Magaña S., Breeding C.M., Sohrabi S., Collins A.T. (2024b) Spectroscopic characterization of rare natural pink diamonds with yellow color zones. *Diamond and Related Materials*, Vol. 148, article no. 111428, <http://dx.doi.org/10.1016/j.diamond.2024.111428>
- Laidlaw F.H.J., Diggle P.L., Breeze B.G., Dale M.W., Fisher D., Bealand R. (2021) Spatial distribution of defects in a plastically deformed natural brown diamond. *Diamond and Related Materials*, Vol. 117, article no. 108465, <http://dx.doi.org/10.1016/j.diamond.2021.108465>
- Lenz C., Belousova E., Lumpkin G.R. (2020) The in-situ quantification of structural radiation damage in zircon using laser-induced confocal photoluminescence spectroscopy. *Minerals*, Vol. 10, No. 1, article no. 83, <http://dx.doi.org/10.3390/min10010083>
- Liaugaudas G., Collins A.T., Suhling K., Davies G., Heintzmann R. (2009) Luminescence-lifetime mapping in diamond. *Journal of Physics: Condensed Matter*, Vol. 21, No. 36, article no. 364210, <http://dx.doi.org/10.1088/0953-8984/21/36/364210>
- Liaugaudas G., Davies G., Suhling K., Khan R.U.A., Evans D.J.F. (2012) Luminescence lifetimes of neutral nitrogen-vacancy centres in synthetic diamond containing nitrogen. *Journal of Physics: Condensed Matter*, Vol. 24, No. 43, article no. 435503, <http://dx.doi.org/10.1088/0953-8984/24/43/435503>
- Lim H., Park S., Cheong H., Choi H.-M., Kim Y.C. (2010) Discrimination between natural and HPHT-treated type IIa diamonds using photoluminescence spectroscopy. *Diamond and Related Materials*, Vol. 19, No. 10, pp. 1254–1258, <http://dx.doi.org/10.1016/j.diamond.2010.06.007>
- Liu Y., Qi L., Schwarz D., Zhou Z. (2022) Color mechanism and spectroscopic thermal variation of pink spinel reportedly from Kuh-i-lal, Tajikistan. *G&G*, Vol. 58, No. 3, pp. 338–353, <http://dx.doi.org/10.5741/GEMS.58.3.338>
- Loudin L.C. (2017) Photoluminescence mapping of optical defects in HPHT synthetic diamond. *G&G*, Vol. 53, No. 2, pp. 180–188, <http://dx.doi.org/10.5741/GEMS.53.2.180>
- Lu H.C., Peng Y.C., Lin M.Y., Chou S.L., Lo J.L., Cheng B.M. (2017) Analysis of boron in diamond with UV photoluminescence. *Carbon*, Vol. 111, pp. 835–838, <http://dx.doi.org/10.1016/j.carbon.2016.10.082>
- Malsy A.-K., Karampelas S., Schwarz D., Klemm L., Armbruster T., Tuan D.A. (2012) Orangy-red to orangy-pink gem spinels from a new deposit at Lang Chap (Tan Huong-Truc Lau), Vietnam. *Journal of Gemmology*, Vol. 33, No. 1–4, pp. 19–27.
- Martineau P.M., McGuinness C.D. (2018) De Beers consumer confidence technical research and diamond verification instruments. In *Diamonds—Source to Use Conference* pp. 35–43, <https://www.saimm.co.za/Conferences/Diamonds2018/035-Martineau.pdf>
- McGuinness C.D., Wassell A.M., Lanigan P.M.P., Lynch S.A. (2020) Separation of natural from laboratory-grown diamond using time-gated luminescence imaging. *G&G*, Vol. 56, No. 2, pp. 220–229, <http://dx.doi.org/10.5741/GEMS.56.2.220>
- Mikhailik V.B., Kraus H., Wahl D., Mykhaylyk M.S. (2005) Luminescence studies of Ti-doped Al₂O₃ using vacuum ultraviolet synchrotron radiation. *Applied Physics Letters*, Vol. 86, No. 10, article no. 101909, <http://dx.doi.org/10.1063/1.1880451>
- Monticone D.G., Quercioli F., Mercatelli R., Soria S., Borini S., Poli T., Vannoni M., Vittone E., Olivero P. (2013) Systematic study of defect-related quenching of NV luminescence in diamond with time-correlated single-photon counting spectroscopy. *Physical Review B*, Vol. 88, No. 15, article no. 155201, <http://dx.doi.org/10.1103/PhysRevB.88.155201>
- Nagabhushana H., Prashantha S.C., Lakshminarasappa B.N., Singh F. (2008) Ionoluminescence and photoluminescence studies of Ag⁺ ion irradiated kyanite. *Journal of Luminescence*, Vol. 128, No. 1, pp. 7–10, <http://dx.doi.org/10.1016/j.jlumin.2007.04.010>
- Nasdala L., Götz J., Hanchar J.M., Gaft M., Krbetschek R. (2004) Luminescence techniques in earth sciences. In A. Beran and E. Libowitzky, Eds., *Spectroscopic Methods in Mineralogy*. European Mineralogical Union, Vol. 6, pp. 43–92.
- Nasdala L., Beyssac O., Schopf W., Bleisteiner B. (2012) Application of Raman-based images in the earth sciences. In A. Zoubir, Ed.,

- Raman Imaging—Techniques and Applications*. Springer Series in Optical Sciences, No. 168, Springer-Verlag, Berlin and Heidelberg, pp. 145–187.
- Nichols E.L., Howes H.L., Wilber D.T. (1918) The photoluminescence and cathodo-luminescence of calcite. *Physical Review*, Vol. 12, No. 5, pp. 351–367, <http://dx.doi.org/10.1103/PhysRev.12.351>
- Noguchi N., Abduriyim A., Shimizu I., Kamegata N., Odake S., Kagi H. (2013) Imaging of internal stress around a mineral inclusion in a sapphire crystal: Application of micro-Raman and photoluminescence spectroscopy. *Journal of Raman Spectroscopy*, Vol. 44, No. 1, pp. 147–154, <http://dx.doi.org/10.1002/jrs.4161>
- O'Donnell K.P., Marshall A., Yamaga M., Henderson B., Cockayne B. (1989) Vibronic structure in the photoluminescence spectrum of Cr³⁺ ions in garnets. *Journal of Luminescence*, Vol. 42, No. 6, pp. 365–373, [http://dx.doi.org/10.1016/0022-2313\(89\)90081-1](http://dx.doi.org/10.1016/0022-2313(89)90081-1)
- Pegasus Overseas Limited, Lazare Kaplan International, General Electric Company—press release (1999) Diamonds.net, March 25.
- Prasad A.K., Jain M. (2018) Dynamics of the deep red Fe³⁺ photoluminescence emission in feldspar. *Journal of Luminescence*, Vol. 196, pp. 462–469, <http://dx.doi.org/10.1016/j.jlumin.2017.11.051>
- Read P.G. (2008) *Gemmology*, 3rd ed. Elsevier Butterworth-Heinemann, Oxford, UK.
- Saeseaw S., Wang W., Scarratt K., Emmett J.L., Douthit T.R. (2009) Distinguishing heated spinels from unheated natural spinels and from synthetic spinels. *GIA Research News*, <http://www.gia.edu/gia-news-research-NR32209A>
- Seat H.C., Sharp J.H. (2004) Dedicated temperature sensing with c-axis oriented single-crystal ruby (Cr³⁺: Al₂O₃) fibers: Temperature and strain dependences of R-line fluorescence. *IEEE Transactions on Instrumentation and Measurement*, Vol. 53, No. 1, pp. 140–154, <http://dx.doi.org/10.1109/TIM.2003.822010>
- Shigley J., Moses T., McClure S., Van Dael M. (1999) GIA reports on GE POL diamonds. *Rapaport Diamond Report*, Vol. 22, No. 36, pp. 1, 11, 14, 18.
- Shinno I. (1987) Color and photo-luminescence of rare earth element-doped zircon. *Mineralogical Journal*, Vol. 13, No. 5, pp. 239–253, <http://dx.doi.org/10.2465/minerj.13.239>
- Simpson C.T., Imano W., Becker W.M. (1980) Photoluminescence, optical absorption, and excitation spectra of cinnabar (α-HgS). *Physical Review B*, Vol. 22, No. 2, pp. 911–920, <http://dx.doi.org/10.1103/PhysRevB.22.911>
- Smith C.P., Bosshart G., Ponahlo J., Hammer V M., Klapper H., Schmetzer K. (2000) GE POL diamonds: Before and after. *G&G*, Vol. 36, No. 3, pp. 192–215, <http://dx.doi.org/10.5741/GEMS.36.3.192>
- Smith C.P., McClure S.F., Eaton-Magaña S., Kondo D.M. (2007) Pink-to-red coral: A guide to determining origin of color. *G&G*, Vol. 43, No. 1, pp. 4–15, <http://dx.doi.org/10.5741/GEMS.43.1.4>
- Smith E.M., Krebs M.Y., Genzel P.T., Brenker F.E. (2022) Raman identification of inclusions in diamond. *Reviews in Mineralogy and Geochemistry*, Vol. 88, pp. 451–473, <http://dx.doi.org/10.2138/rmg.2022.88.08>
- Solin S.A. (1972) Photoluminescence of natural type I and type IIb diamonds. *Physics Letters A*, Vol. 38, No. 2, pp. 101–102, [http://dx.doi.org/10.1016/0375-9601\(72\)90506-3](http://dx.doi.org/10.1016/0375-9601(72)90506-3)
- Song Z., Lu T., Lan Y., Shen M., Ke J., Liu J., Zhang Y. (2012) The identification features of undisclosed loose and mounted CVD synthetic diamonds which have appeared recently in the NGTC laboratory. *Journal of Gemmology*, Vol. 33, No. 1-4, pp. 45–48.
- Stachel T., Luth R.W. (2015) Diamond formation—Where, when and how? *Lithos*, Vol. 220-223, pp. 200–220, <http://dx.doi.org/10.1016/j.lithos.2015.01.028>
- Thomaz M.F., Davies G. (1978) The decay time of N3 luminescence in natural diamond. *Proceedings of the Royal Society A*, Vol. 362, No. 1710, pp. 405–419, <http://dx.doi.org/10.1098/rspa.1978.0141>
- Thompson D.B., Kidd J.D., Åström M., Scarani A., Smith C.P. (2014) A comparison of R-line photoluminescence of emeralds from different origins. *Journal of Gemmology*, Vol. 34, No. 4, pp. 334–343.
- Thompson D.B., Bayens C.J., Morgan M.B., Myrick T.J., Sims N.E. (2017) Photoluminescence spectra of emeralds from Colombia, Afghanistan, and Zambia. *G&G*, Vol. 53, No. 3, pp. 296–311, <http://dx.doi.org/10.5741/GEMS.53.3.296>
- Tsai T.-H. (2023) Imaging-assisted Raman and photoluminescence spectroscopy for diamond jewelry identification and evaluation. *Applied Optics*, Vol. 62, No. 10, pp. 2587–2594, <http://dx.doi.org/10.1364/AO.484366>
- Tsai T.-H., D'Haenens-Johansson U.F.S. (2021) Rapid gemstone screening and identification using fluorescence spectroscopy. *Applied Optics*, Vol. 60, No. 12, pp. 3412–3421, <http://dx.doi.org/10.1364/AO.419885>
- Tsai T.-H., Takahashi H. (2022) Automatic jewelry identification and evaluation based on imaging-assisted Raman spectroscopy. In C.F. Hahlweg and J.R. Mulley, Eds., *Novel Optical Systems, Methods, and Applications XXV*. SPIE, Bellingham, Washington, pp. 49–57.
- Tsai T.-H., Zhou C. (2020) Lab Notes: Fluorescence spectroscopy for colored pearl treatment screening. *G&G*, Vol. 56, No. 1, pp. 136–137.
- (2021) Rapid detection of color-treated pearls and separation of pearl types using fluorescence analysis. *Applied Optics*, Vol. 60, No. 20, pp. 5837–5845, <http://dx.doi.org/10.1364/AO.427203>
- Turnier R.B. (2022) Views on corundum genesis from zircon inclusions, SIMS oxygen isotope analyses, geochronology, trace elements, and spectroscopy. PhD thesis, University of Wisconsin-Madison.
- Vigier M., Massuyeau F., Fritsch E. (2024) Orange luminescence of α-Al₂O₃ related to clusters consisting of F centers and divalent cations. *Luminescence*, Vol. 39, No. 5, article no. e4757, <http://dx.doi.org/10.1002/bio.4757>
- Vuong B.T.S., Osanai Y., Lenz C., Nakano N., Adachi T., Belousova E., Kitano I. (2019) Gem-quality zircon megacrysts from placer deposits in the central highlands, Vietnam—Potential source and links to Cenozoic alkali basalts. *Minerals*, Vol. 9, No. 2, article no. 89, <http://dx.doi.org/10.3390/min9020089>
- Walker J. (1977) An optical study of the TR12 and 3H defects in irradiated diamond. *Journal of Physics C: Solid State Physics*, Vol. 10, No. 16, pp. 3031–3037, <http://dx.doi.org/10.1088/0022-3719/10/16/013>
- Wang W., Scarratt K., Hyatt A., Shen A.H.-T., Hall M. (2006) Identification of “chocolate pearls” treated by Ballerina Pearl Co. *G&G*, Vol. 42, No. 4, pp. 222–235, <http://dx.doi.org/10.5741/GEMS.42.4.222>
- Wang W., Hall M.S., Moe K.S., Tower J., Moses T.M. (2007) Latest-generation CVD-grown synthetic diamonds from Apollo Diamond Inc. *G&G*, Vol. 43, No. 4, pp. 294–312, <http://dx.doi.org/10.5741/GEMS.43.4.294>
- Wang W., D'Haenens-Johansson U.F.S., Johnson P., Moe K.S., Emerson E., Newton M.E., Moses T.M. (2012) CVD synthetic diamonds from Gemesis Corp. *G&G*, Vol. 48, No. 2, pp. 80–97, <http://dx.doi.org/10.5741/GEMS.48.2.80>
- Wang Z., Tsai T.-H., Wang W. (2023) Excimer laser based photoluminescence device for diamond identification. In *Novel Optical Systems, Methods, and Applications XXVI*, Vol. 12665. SPIE, pp. 118–122, <http://dx.doi.org/10.1117/12.2672542>
- Waychunas G.A. (2014) Luminescence spectroscopy. In G.S. Henderson et al., *Reviews in Mineralogy and Geochemistry*, Vol. 78. Mineralogical Society of America, Chantilly, Virginia, pp. 175–211.
- Wong W.C., McClure D.S., Basun S.A., Kokta M.R. (1995) Charge-exchange processes in titanium-doped sapphire crystals. I. Charge-exchange energies and titanium-bound excitations. *Physical Review B*, Vol. 51, No. 9, pp. 5682–5698, <http://dx.doi.org/10.1103/PhysRevB.51.5682>
- Wotherspoon A., Steeds J.W., Catmull B., Butler J. (2003) Photolu-

- minescence and positron annihilation measurements of nitrogen doped CVD diamond. *Diamond and Related Materials*, Vol. 12, pp. 652–657, [http://dx.doi.org/10.1016/S0925-9635\(02\)00229-7](http://dx.doi.org/10.1016/S0925-9635(02)00229-7)
- Wu J., Sun X., Ma H., Ning P., Tang N., Ding T., Li H., Zhang T., Ma Y. (2023) Purple-violet gem spinel from Tanzania and Myanmar: Inclusion, spectroscopy, chemistry, and color. *Minerals*, Vol. 13, No. 2, article no. 226, <http://dx.doi.org/10.3390/min13020226>
- Xu W., Tsai T.-H., Palke A. (2023) Study of 405 nm laser-induced time-resolved photoluminescence spectroscopy on spinel and alexandrite. *Minerals*, Vol. 13, No. 3, article no. 419, <http://dx.doi.org/10.3390/min13030419>
- Yelissev A.P., Khrenov A.Y., Afanasiev V.P. (2016) Photoluminescence spectra of impact diamonds formed by solid-state graphite-to-diamond transition. *Journal of the Optical Society of America B*, Vol. 33, No. 3, pp. B43–B48, <http://dx.doi.org/10.1364/JOSAB.33.000B43>
- Yu H., Clarke D.R. (2002) Effect of codoping on the R-line luminescence of Cr³⁺-doped alumina. *Journal of the American Ceramic Society*, Vol. 85, No. 8, pp. 1966–1970, <http://dx.doi.org/10.1111/j.1151-2916.2002.tb00389.x>
- Zaitsev A.M. (2001) *Optical Properties of Diamond: A Data Handbook*. Springer-Verlag, Berlin.
- Zaitsev A.M., Kazuchits N.M., Moe K.S., Butler J.E., Korolik O.V., Rusetsky M.S., Kazuchits V.N. (2021) Luminescence of brown CVD diamond: 468 nm luminescence center. *Diamond and Related Materials*, Vol. 113, article no. 108255, <http://dx.doi.org/10.1016/j.diamond.2021.108255>
- Zeug M., Vargas A.I.R., Nasdala L. (2017) Spectroscopic study of inclusions in gem corundum from Mercaderes, Cauca, Colombia. *Physics and Chemistry of Minerals*, Vol. 44, No. 3, pp. 221–233, <http://dx.doi.org/10.1007/s00269-016-0851-4>
- Zeug M., Nasdala L., Chutimun C.N., Hauzenberger C. (2022) Gem topaz from the Schneckenstein Crag, Saxony, Germany: Mineralogical characterization and luminescence. *G&G*, Vol. 58, No. 1, pp. 2–17, <http://dx.doi.org/10.5741/GEMS.58.1.2>
- Zhang Z., Ye M., Shen A.H. (2019) Characterisation of peridot from China's Jilin Province and from North Korea. *Journal of Gemmology*, Vol. 36, No. 5, pp. 436–446.
- Zhang Z., Shen A. (2023) Fluorescence and phosphorescence spectroscopies and their applications in gem characterization. *Minerals*, Vol. 13, No. 5, article no. 626, <http://dx.doi.org/10.3390/min13050626>
- Zhou C., Homkrajae A., Ho J.W.Y., Hyatt A., Sturman N. (2012) Update on the identification of dye treatment in yellow or “golden” cultured pearls. *G&G*, Vol. 48, No. 4, pp. 284–291, <http://dx.doi.org/10.5741/GEMS.48.4.284>
- Zhou C., Ho J.W.Y., Chan S., Zhou J.Y., Wong S.D., Moe K.S. (2016) Identification of “pistachio” colored pearls treated by Ballerina Pearl Co. *G&G*, Vol. 52, No. 1, pp. 50–59, <http://dx.doi.org/10.5741/GEMS.52.1.50>
- Zhou C., Tsai T.-H., Sturman N., Nilpetploy N., Manustrong A., Lawanwong K. (2020) Optical whitening and brightening of pearls: A fluorescence spectroscopy study. *G&G*, Vol. 56, No. 2, pp. 258–265, <http://dx.doi.org/10.5741/GEMS.56.2.258>

For online access to all issues of GEMS & GEMOLOGY from 1934 to the present, visit:

gia.edu/gems-gemology

